Microbial Safety Verification on an Infusion Set for Contrast Enhanced Imaging

Marlein Miranda Cona[1], Walter Coudyzer[1], Yuanbo Feng[1], Feng Chen[1], Alfons Verbruggen[2], Raymond Oyen[1] and Yicheng Ni[1]

[1]Radiology Section, Department of Imaging & Pathology; [2]Laboratory of Radiopharmacy, Faculty of Pharmaceutical Sciences. Biomedical Sciences Group, K.U.Leuven, Belgium

Abstract

Multiple uses of automatic contrast injection systems may impose septic risks on patients. The purpose of this study was to check whether a newly developed replaceable patient-delivery system may allow multiple uses of the system but without such risks. The experiment was conducted on rabbits with intravenous injection of ^{99m}Tc-dimercaptopropionyl-human serum albumin (^{99m}Tc-DMP-HSA). The tracer was monitored by sampling the delivery system for checking if the radiotracer from the patient line in contact with blood is able to cross the safety zone and reach the dual-syringe injector system. The tested patient-delivery system proves convenient and safe.

Introduction

Automatic contrast injection systems are used for delivery of contrast media during enhanced imaging procedures. But, accidental patient cross contaminations with microbial flora and pathogens associated with infectious diseases may occur. To prevent this limitation, the injection system including the power syringes and filling & injecting set has to be changed for each patient. However, this proves expensive and time consuming owing to the wasted contrast materials left over in the setup from each exam, the growing consumptions of disposable devices, and the prolonged pauses for replacing the entire set-up with each patient. More institutions worldwide have been applying multiple usages of the syringes with automatic injectors for serial patients. Commercially available injection systems containing a special one-way-valve tube device have been mostly used. Nevertheless, nosocomial infections between patients have been reported.

Transflux™ is a patient-delivery system that contains a safety zone composed by a length of tubing and two one-way valves. It permits to flush the delivery system and the vein but prevents blood reflux during contrast-enhanced imaging. This system is replaced for each new patient, whereas the power syringes need to be changed only once a day after multiple uses for a series of patients. It has been applied for several years in many radiology units without any contaminative infections reported. To verify the microbial safety of Transflux™ system and to justify its current clinical use, we performed this experiment in rabbits with intravenous injection of a diffusible radiotracer.

Methods & Materials

Twelve Transflux™ patient-delivery systems (Dipenbeek, Belgium) were tested according to a multiple-use approach using an automatic contrast injection system consisting of dual syringes and one filling & injecting set. Two protocols with normal saline only (n=6) or contrast media plus normal saline (n=6) loaded in the injection system were performed. Each patient-delivery system was connected through an infusion catheter to the ear vein of a rabbit that was intravenously pre-injected with ^{99m}Tc-dimercaptopropionyl-human serum albumin (^{99m}Tc-DMP-HSA). Aliquots were sampled from the filling & injecting set, patient line and animal blood for radioactive analysis after the replacement of each patient-delivery system.

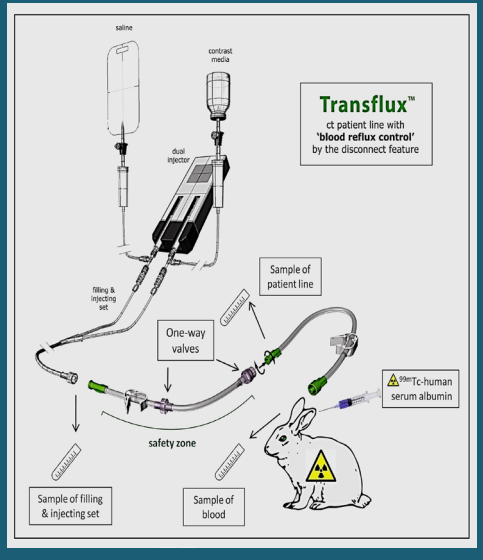

^{99m}Tc-DMP-HSA is a diffusible radiotracer with molecular size (~14 nm) comparable to those of small pathogens.

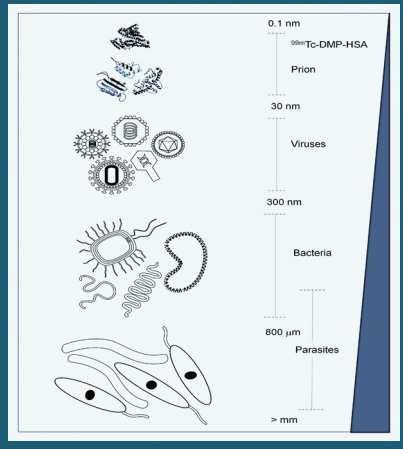

Results

For the protocol performed using only normal saline, radioactivity was found in the blood circulation of the rabbit (1655903 ± 593221 CPM) and in the patient line (52894 ± 33080 CPM) but in none of samples from the filling & injecting set (8 ± 3 CPM), relative to the background (7 ± 3 CPM) (p = 0.726).

Experimental results attained using contrast plus saline show radioactivity in the blood circulation of the rabbit (1119107± 183174 CPM) and in the patient line (32991 ± 20232 CPM) but in none of samples from the filling & injecting set (6 ± 6 CPM), relative to the background (6 ± 4 CPM) (p = 0.955).

		Animal blood (0.2 mL) CPM (n = 6)	Patient line CPM (n = 6)	Filling ☒ injecting set CPM (n = 6)	Natural background radiation CPM (n = 6)
		Before Safety zone		After Safety zone	
protocol	Samples	2056151	88259	6	6
		2580793	36427	5	5
		1411901	95484	11	13
		1707872	30787	7	5
		1230304	12328	5	4
		948399	54081	12	9
	Mean	**1655903**	**52894**	**8**	**7**
	SD	593221	33080	3	3
	p values	Filling ☒injecting set vs. Natural background			**0.726**
		Patient line vs. Natural background radiation			0.003
		Animal blood vs. Natural background radiation			☒.0001
		Filling ☒injecting set vs. Patient line			**0.003**
		Filling ☒injecting set vs. Animal blood			☒.0001
		Patient line vs. Animal blood			☒.0001
Contrast protocol	Samples	1269190	60928	5	9
		1401743	52357	7	12
		1067618	14303	2	0
		1086509	10062	5	6
		965634	30246	0	3
		923948	30052	16	4
	Mean	**1119107**	**32991**	**6**	**6**
	SD	183174	20232	6	4
	p values	Filling ☒injecting set vs. Natural background			**0.955**
		Patient line vs. Natural background radiation			0.003
		Animal blood vs. Natural background radiation			☒.0001
		Filling ☒injecting set vs. Patient line			**0.003**
		Filling ☒injecting set vs. Animal blood			☒.0001
		Patient line vs. Animal blood			☒.0001

Conclusions

This study proves the convincing advantage of using the Transflux™ patient-delivery system in terms of microbial safety and cost-benefits. This system allows safe multiple use of the automatic injector system for several patients without risk of contamination and extravasation but with improved clinical efficiency. It reduces unnecessary waste of contrast media with each patient procedure and of the costly automatic injector systems.

Study on the Microbial Safety of an Infusion Set for Contrast-Enhanced Imaging

Marlein Miranda Cona, BSc, Matthias Bauwens, PhD,† Yichao Zheng, BSc,* Walter Coudyzer, BSc,* Junjie Li, MD,* Yuanbo Feng, MD,* Huaijun Wang, MD, PhD,* Feng Chen, MD, PhD,* Alfons Verbruggen, PhD,† Raymond Oyen, MD, PhD,* and Yicheng Ni, MD, PhD**

Objectives: Multiple uses of automatic contrast injection systems may impose septic risks on patients. The purpose of this experiment was to verify whether a newly developed replaceable patient-delivery system may allow multiple uses of the system but without such risks.

Methods: Twelve patient-delivery systems were tested according to a multiple-use approach using an automatic contrast injection system consisting of dual syringes and one filling and injecting set. Two protocols with normal saline only (n = 6) or contrast media plus normal saline (n = 6) loaded in the injection system were performed. Each patient-delivery system was connected through an infusion catheter to the ear vein of a rabbit that was intravenously preinjected with a diffusible radiotracer ^{99m}Tc-dimercaptopropionyl-human serum albumin. Aliquots were sampled from the filling and injecting set, patient line, and animal blood for radioactive analysis after the replacement of each patient-delivery system.

Results: For the protocol performed using only normal saline, radioactivity was found in the blood circulation of the rabbit (1655903 ± 593221 CPM) and in the patient line (52894 ± 33080 CPM), but, virtually, in none of samples from the filling and injecting set (8 ± 3 CPM), relative to the background (7 ± 3 CPM) (P = 0.726). Similarly, experimental results attained using contrast plus saline show radioactivity in the blood circulation of the rabbit (1119107 ± 183174 CPM) as well as in the patient line (32991 ± 20232 CPM) but in none of samples from the filling and injecting set (6 ± 6 CPM), relative to the background (6 ± 4 CPM) (P = 0.955).

Conclusions: The tested patient-delivery system proves convenient and safe. It allows multiple uses of the contrast injection system and avoids the risk of cross contamination.

Key Words: automatic injector, contrast media, CT, MRI, microbiological contamination

(*Invest Radiol* 2012;47: 247–251)

Automatic contrast injection systems are widely used for robotic delivery of contrast media during enhanced imaging procedures with different modalities[1,2] such as computed tomography (CT), magnetic resonance imaging (MRI), and angiography. However, accidental patient cross contaminations with microbial flora (eg, coagulase-negative staphylococci) and bloodborne pathogenic microorganisms (viruses, bacteria, parasites, etc) associated with infectious diseases such as malaria, acquired immune deficiency syndrome, hepatitis C, and hepatitis B have been reported.[3–5] Potential outbreak of proteinaceous infectious particles transmission also remains a concern, which can cause incurable neurodegenerative disorders in humans known as transmissible spongiform encephalopathies.[6–8] To prevent possible nosocomial infections, the injection system including the power syringes and filling and injecting set has to be entirely changed for each patient.

Regulatory authorities such as the Food and Drug Administration in the United States and the Federal Institute for Drugs and Medical Devices in Germany have imposed restrictions over the syringes, tubing, and connectors from contrast injectors as single-use devices[9,10] in accordance with the instructions from manufacturers' advertisements and clinical uses. However, this implementation proves expensive and time consuming owing to the wasted contrast materials left over in the setup from each examination, the growing consumptions of disposable devices, and the prolonged pauses for replacing the entire set-up with each patient.

To counteract such drawbacks, Canada Health performed a study to assess the safety level and feasibility of multiple patient dosages of the costly contrast materials.[11] Results showed that the transfer devices having dedicated check valves can prevent backflow of potentially contaminating body fluids in a multidosing contrast media delivery setting. As cost-effective alternative, the same dual-head injector set-up could be used for up to 4 hours, and just the patient tube needed replacement for each case. After that period the complete set-up should be substituted.[11] Gradually more institutions worldwide have been applying multiple usages of the syringes with automatic injectors for serial patients to reduce material and labor costs. Commercially available injection systems containing a special one-way valve tube device have been mostly used. Nevertheless, nosocomial infections among patients have been reported as a result of contamination of the injection system with bloodborne pathogens.[12]

Transflux is a patient-delivery system produced by P&R MEDICAL (Diepenbeek, Belgium)[13] (Fig. 1). It incorporates a safety zone composed by a length of tubing and 2 one-way valves that permit to flush the delivery system and the vein but prevents blood reflux during contrast-enhanced imaging procedures. This system is replaced for each new patient, while the power syringes need to be changed only once a day after multiple uses for a series of patients. It has been applied for several years in many radiology departments without any contaminative infections reported. To verify the safety of Transflux system and to justify its current clinical use, we conducted this experiment in rabbits with intravenous injection of a diffusible radioactive compound ^{99m}Tc-dimercaptopropionyl-human serum albumin (^{99m}Tc-DMP-HSA). Once injected

Received June 13, 2011, and accepted for publication (after revision) October 4, 2011.

From the *Radiology Section, Department of Imaging and Pathology, Biomedical Sciences Group, University of Leuven, Belgium; and †Laboratory of Radiopharmacy, Faculty of Pharmaceutical Sciences, University of Leuven, Belgium.

Supported in part by the K.U. Leuven Molecular Small Animal Imaging Center MoSAIC (KUL EF/05/08); the center of excellence in vivo molecular imaging research of K.U. Leuven; KU Leuven project IOF-HB/08/009; and the European Union (Asia-Link CfP 2006-EuropeAid/123738/C/ACT/Multi-Proposal No. 128–498/111).

The contents of this paper are the sole responsibility of Leuven University, Belgium and can under no circumstances be regarded as reflecting the position of the European Union.

The corresponding author is currently a Bayer Lecture Chair holder.

Conflicts of interest and sources of funding: none declared.

Reprints: Yicheng Ni, MD, PhD, Radiology Section, University Hospitals, K.U. Leuven, Herestraat 49, B-3000, Leuven, Belgium. E-mail: yicheng.ni@med.kuleuven.be.

ISSN: 0020-9996/12/4704-0247

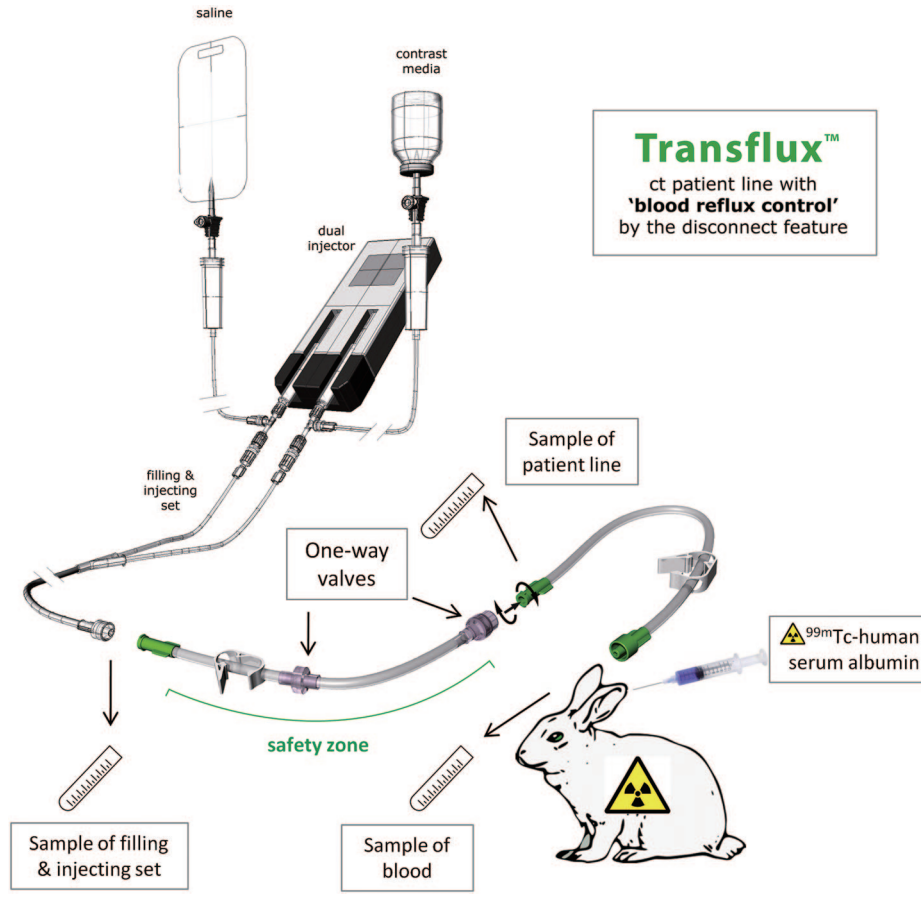

FIGURE 1. Schematic representation of the Transflux CT patient delivery system (P&R Medical company) composed of a "safety zone" tube containing 2 one-way valves, which is connected on one side to the dual-injector system through the injecting and filling set and on the other side to the patient line. In vivo experiments for safety evaluation were done in normal rabbits with intravenous injection of ^{99m}Tc-DMP-HSA as radiotracer. Samples from the filling and injecting set, patient line, and animal blood were collected for radioactive analyses.

in a patient or animal, it remains largely in the blood pool.[14] The tracer was monitored by sampling the delivery system for checking whether the radioactive compound (simulating infectious pathogens) from the patient line in tight contact with animal bloodstream is able to cross the safety zone and reach the dual-syringe injector system.

MATERIALS AND METHODS

This animal study was approved by the institutional ethics and radioprotection committees. To simulate normal clinical scenario, the studies were performed using a power injector (Dual Shot GX; Nemoto Kyorindo, Tokyo, Japan) comprising 2 disposable syringes, one of 200 mL for contrast media infusion and the other of 100 mL for normal saline flushing, both coupled to each other and to a filling and injecting set through a T-connector.

Twelve Transflux CT patient-delivery systems of PR-21414–100 cm type GHB (P&R Medical company, Diepenbeek, Belgium) were tested according to the following 2 protocols:

(*a*) Multiple uses of disposable syringes filled with saline solution (Protocol A)—Both disposable syringes were filled with saline solution for further filling of several infusion sets (n = 6).
(*b*) Multiple uses of disposable syringes filled with contrast agent and saline solution in 2 separate power syringes (Protocol B), taking different viscosity into account—For simulating normal clinical conditions, one syringe was loaded with Iomeron 350 media (Iodinated contrast medium Iomeprol, Bracco, Konstanz, Germany) and the other with saline solution. After filling with media in each delivery system, a volume of 100 mL of saline was pushed through the line (n = 6).

The experiments were performed using normal white male New Zealand rabbits (n = 2) weighing around 5.0 kg (Animal House, K.U. Leuven, Belgium). The animal was sedated by intramuscular administration of Ketalar (ketamine hydrochloride, Parke-Davis Warner-Lambert, Bornem, Belgium) and Ranpun (xylazine hydrochloride, Bayer AG, Leverkusen, Germany) at 0.5 mL/kg for both. Then, it was kept under sedation during the experiment using pentobarbital (Nembutal; Sanofi Sante Animale, Brussels, Belgium) intraperitoneally at 60 mg/kg. After fixation and restriction of the sedated rabbit in the supine position using a dedicated holder, a 22-G peripheral venous catheter (0.9 mm × 25 mm, BD Insyte-W, Madrid, Spain) was placed in the marginal vein of both ears. One of them was used for administration of the radiotracer solution and the other for connection of the Transflux patient-delivery system to be tested and for blood withdrawal to control the remaining radioactivity in the animal over time.

A single dose of 370 MBq of ^{99m}Tc-DMP-HSA (Fig. 2) was prepared as previously described[12] and administered to the animal. Then, the infusion sets previously filled with saline solution or contrast medium along with saline solution was coupled to the contralateral catheter in such a way as to guarantee a contact between the solution and the animal blood without air in-between. Taking into account that an actual scan only takes a few minutes, the animal was left in connection with the patient line for 10 minutes. After that period, the patient line was carefully disconnected from the animal. After each sampling and installation of a new set, 10 mL was flushed to challenge the valves and to ensure the patency of venous line.

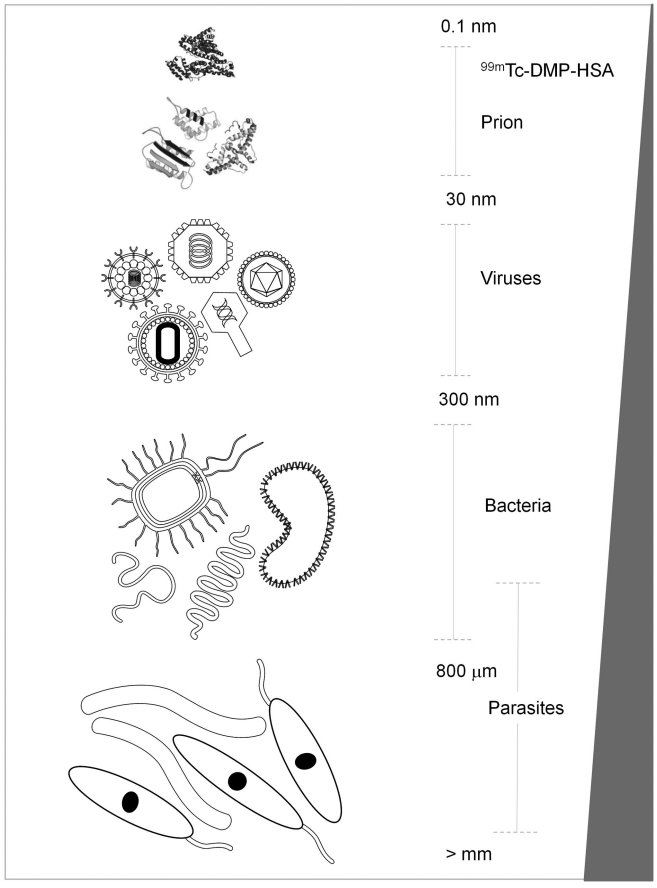

FIGURE 2. Schematic representation of the size and shape of different infectious pathogens including prions, viruses, bacteria, and parasites in relation to the ^{99m}Tc-DMP-HSA radiotracer. Units of length: 1.0 mm = 1000 μm, 1.0 μm = 1000 nm.

An aliquot of 10 mL as well as the whole content of 3.5 mL was collected by tapping from the opening end of the filling and injecting set and patient line, respectively (Fig. 1). Their radioactivities were counted for 1 minute (Counts per minute: CPM). Animal blood samples (~200 μL) were withdrawn for controlling the circulating activity during each test. Radioactivity measurements of the collected samples mounted in a sample changer (Wallac 1480 Wizard 3, Wallac, Turku, Finland) were done using a gamma counter (3-in. NaI(Tl) well crystal) coupled to a multichannel analyzer. Rabbits were observed for life signs for 1 week.

Statistical analyses were carried out using GraphPad Prism V.3 software (GraphPad Software Inc., San Diego, CA). Numerical data of measured radioactivities were expressed as mean ± SD and compared between injector syringe set and natural background radiation using 2-tailed Student *t* test. A statistical significance was considered at a probability value smaller than 0.05.

RESULTS

The rabbits tolerated well the experimental procedures including sedation, anesthesia, catheterization of marginal ear veins, tracer injection, and the multiple samplings over 3 hours per protocol, and recovered to normal status afterward.

The patient delivery systems were tested according to 2 protocols: (1) multiple uses of disposable syringes filled with saline solution, and (2) multiple uses of the 2 disposable syringes one filled with contrast solution and the other one with saline solution. After connecting each patient line to a rabbit, which was intravenously injected with ^{99m}Tc-DMP-HSA, samples collected from the filling and injecting set and patient line were counted for radioactivity in comparison with natural background.

The results obtained from saline and saline plus contrast protocols are shown in Table 1. For saline protocol, radioactivity detected in the blood circulation of the rabbit (1655903 ± 593221 CPM per 0.2 mL blood) was statistically higher than that (52894 ± 33080 CPM) in the patient line ($P < 0.0001$). Actually there was no radioactivity detected from the filling and injecting set in comparison to the patient line across the safety zone ($P = 0.003$). There were no significant differences between the radioactivity in the samples (8 ± 3 CPM) from filling and injecting set and the natural background radiation (7 ± 3 CPM) ($P = 0.726$).

Likewise, in the contrast agent protocol, there were significant differences between the radioactivity detected in the blood circulation of the animal (1119107 ± 183174 CPM per 0.2 mL blood) and the patient line (32991 ± 20232 CPM); ($P < 0.0001$). No radioactivity was found in any samples from the filling and injecting set (6 ± 6 CPM) in great contrast to the patient line across the safety zone ($P = 0.003$). Statistically, there were no significant differences between samples from filling and injecting set (6 ± 6 CPM) and natural background radiation (6 ± 4 CPM; $P = 0.955$).

DISCUSSION

For avoiding risk of cross-infections when using automatic injectors, a new injector setup for each new patient has to be used for contrast enhanced imaging examinations in daily routine of a radiology department. However, it increases intervals between examinations and hinders the workflow with ever-increasing numbers of patients. The contrast dose received by each patient constitutes often only a small portion of the total amount of contrast agent loaded in the injector system, leading to a great waste of the unused media. Moreover, the growing number of examinations done per day leads to higher expenditure related to the change of the single-use injection device.

Multiple dosages for more than one patient have been a cost-effective alternative implemented for MRI/CT scans. The high capacity of injection syringes allows successive administrations for multiple cases. Only the device or part in direct contact with the patient, the tubing and connector, is replaced between examinations. This practice can not only reduce the waste of contrast agent and injectors or syringes, but also save the time otherwise consumed by assembling injector and reloading syringes.

Nevertheless, although the patient-line set-up dedicated to contrast administration was used just for a short time period (a few minutes); hygiene studies carried out in experimental and clinical practice have reported cross contamination between patients after the fourth injection.[10]

The Transflux contrast delivery system is a disposable tubing part, which is directly connected by one hand to the patient (i.e.: the CT patient line) and on the other hand to the main injector unit. This system includes a length of tubing (14.5 cm) that contains 2 high quality one-way valves for establishing a fluid connection from the syringe injector system into a patient line but preventing a fluid reflux from the patient line towards the injector system. Such a system with only 1 valve failed to pass the high pressure (4–10 psi or 200–500 mm Hg) in vitro tests (M. M. Cona, personal communication, 2010). In addition, this delivery system is connected with the patient line through a releasable connector. The released position of this releasable connector permits a backflow from the patient during the vein cannulation before connecting to the main injector set, which minimizes extravasations problems. The cost of Transflux

TABLE 1. Results of Measurement of Radioactivity in the Samples From the Experimental Saline and Contrast Plus Saline Protocols as well as the Blood of Experimental Animals

	Before Safety Zone		After Safety Zone	
	Animal Blood (0.2 mL) CPM (n = 6)	**Patient Line CPM (n = 6)**	**Filling and Injecting Set CPM (n = 6)**	**Natural Background Radiation CPM (n = 6)**
Saline protocol				
Samples	2056151	88259	6	6
	2580793	36427	5	5
	1411901	95484	11	13
	1707872	30787	7	5
	1230304	12328	5	4
	948399	54081	12	9
Mean	**1655903**	**52894**	**8**	**7**
SD	593221	33080	3	3
P	Filling and injecting set vs. natural background radiation			**0.726**
	Patient line vs. natural background radiation			0.003
	Animal blood vs. natural background radiation			<0.0001
	Filling and injecting set vs. patient line			**0.003**
	Filling and injecting set vs. animal blood			<0.0001
	Patient line vs. animal blood			<0.0001
Contrast protocol				
Samples	1269190	60928	5	9
	1401743	52357	7	12
	1067618	14303	2	0
	1086509	10062	5	6
	965634	30246	0	3
	923948	30052	16	4
Mean	**1119107**	**32991**	**6**	**6**
SD	183174	20232	6	4
P	Filling and injecting set vs. natural background radiation			**0.955**
	Patient line vs. natural background radiation			0.003
	Animal blood vs. natural background radiation			<0.0001
	Filling and injecting set vs. patient line			**0.003**
	Filling and injecting set vs. animal blood			<0.0001
	Patient line vs. animal blood			<0.0001

SD indicates standard deviation; CPM, counts per minute.

contrast delivery system is approximately only one-tenth of that for the entire injector system.

The introduction of the Transflux delivery system as a "safety zone" avoids the need to change power syringes for each patient procedure by eliminating the risk of contamination of the injector system. For successive patient studies, the "safety zone" and the patient line must be changed but the main injector system can be used for multiple examinations.

To evaluate the safety of the Transflux set, in vivo experiments were conducted based on a multiple dosage approach in combination with radioactive tracer techniques to make highly accurate and sensitive real-time analysis.

According to Stokes-Einstein relation, the diffusion process of a diffusive substance across a certain medium is inversely proportional to its radius and to the viscosity of the solvent at certain temperature. In the current study, we used ^{99m}Tc-DMP-HSA, a diffusible radiotracer whose molecular size (~14 nm)[15] is comparable with those of small bloodborne pathogens. For instance, the most infectious units per mass of prions range between particles of 17 to 27 nm.[16,17] The sizes of the common biologic microorganism can vary from 30 to 300 nm for viruses[18] and from 0.2 to 750 μm for bacteria[19] (Fig. 2). In addition, 2 protocols were performed using different fluids commonly applied for radiology applications to evaluate the influence of the viscosity parameter in the diffusion of such microorganisms through the infusion system.

In the first one, both disposable syringes were filled with saline solution for further successive filling of several Transflux sets. To reproduce more closely the clinical practice, a second protocol was performed, in which one of the syringes was filled with contrast agent (7.5 mPa.s at 37°C) and the other with saline solution (1.0 mPa.s at 37°C) for flushing the delivery system after contrast media infusion. After connecting each patient line to a rabbit intravenously preinjected with ^{99m}Tc-DMP-HSA, samples from the filling and injecting set and patient line were collected and analyzed for checking if the safety zone placed between such tubing segments (Fig. 1) is able to prevent completely the radiotracer diffusion from the animal blood to the automatic injector system. As a representative of all CT and MRI contrast media, we chose Iomeron 350 with a viscosity at a relatively higher level relative to that of normal saline, to cover a full viscosity range, hence results of more general implication.

For each protocol, 6 Transflux sets were tested by replacing the safety zone and patient line but without changing the dual-injector system and the filling and injecting set. Results showed no statistically significant difference in radioactivity between samples from the filling and injecting set and natural background radiation under all conditions tested. Indeed, no radioactivity was detected in any sample from the filling and injecting set after testing each Transflux set in great contrast with the high level of activities present in the patient line as well as in the animal blood. Measurement of radioactivity is a very sensitive and quantitative method, allowing detecting radioactive substances at femtomolar level. To our knowledge, similar in vivo studies on the safety of infusion sets for contrast agent administration have not been published in the literature.

The methodology used for validation in this study also appears reliable and accurate and deserves to be applied for validating the safety of other similar devices before it is widely used for multiple patient applications.

CONCLUSION

This study proves the convincing advantage of using the Transflux patient-delivery system in terms of microbial safety and cost-benefits. This system allows safe multiple use of the automatic injector system for several patients without risk of contamination and extravasation but with improved clinical efficiency. In addition, it reduces unnecessary waste of contrast media with each patient procedure and of the costly automatic injector systems.

REFERENCES

1. Nance JW Jr, Henzler T, Meyer M, et al. Optimization of contrast material delivery for dual-energy computed tomography pulmonary angiography in patients with suspected pulmonary embolism. *Invest Radiol*. 2012;47:78–84.
2. Behrendt FF, Jost G, Pietsch H, et al. Computed tomography angiography: the effect of different chaser flow rates, volumes, and fluids on contrast enhancement. *Invest Radiol*. 2011;46:271–276.
3. Pañella H, Rius C, Caylà JA, et al. Transmission of hepatitis C virus during computed tomography scanning with contrast. *Emerg Infect Dis*. 2008;14:333–336.
4. Chen KT, Chen CJ, Chang PY, et al. A nosocomial outbreak of malaria associated with contaminated catheters and contrast medium of a computed tomographic scanner. *Infect Control Hosp Epidemiol*. 1999;20:22–25.
5. Siegel JD, Rhinehart E, Jackson M, et al. *Healthcare Infection Control Practices Advisory Committee 2007 Guideline for Isolation Precautions: Preventing Transmission of Infectious Agents in Healthcare Settings*. Vol 28. Atlanta GA: Centers for Disease Control and Prevention; 2007.
6. Llewelyn C, Hewitt P, Knight R, et al. Possible transmission of variant Creutzfeldt-Jakob disease by blood transfusion. *Lancet*. 2004;363:417–421.
7. Peden A, Head M, Diane L, et al. Preclinical vCJD after blood transfusion in a codon 129 heterozygous patient. *Lancet*. 2004;364:527–529.
8. Wroe SJ, Pal S, Siddique D, et al. Clinical presentation and pre-mortem diagnosis of variant Creutzfeldt-Jakob disease associated with blood transfusion: a case report. *Lancet*. 2006;368:2061–2067.
9. US Food and Drug Administration. "Medical Devices; Reprocessed Single-Use Devices; Termination of Exemptions from Premarket Notification; Requirement for Submission of Validation Data." Docket No. 03N-0161, Federal Register. 2003;68:23139–23148.
10. Buerke B, Mellmann A, Stehling C, et al. Microbiologic contamination of automatic injectors at MDCT: experimental and clinical investigations. *Am J Roengenol*. 2008;191:W283–W287.
11. Public Health Agency of Canada. Preliminary report: biosafety analysis of one-way backflow valves for multiple patient use of low osmolar intravenous contrast solution. *Can Commun Dis Rep*. 1996;22:28–31.
12. Cantin V, Labadie R, Rhainds M, et al. Intravenous contrast medium administration in computerized axial tomography at the CHUQ Medical Imaging Department [Internet]. Quebec (QC): Centre hospitalier universitaire de Québec (CHUQ). May 14, 2007. Available at: http://www.chuq.qc.ca/NR/rdonlyres/03BC97EF-5F04–4375-BC48–3852965A4EDD/0/R%C3%89SUM%C3%89substancedecontrasteVArevised_VF.pdf. Accessed November 29, 2010.
13. Peters JP. Contrast fluid delivery system. PCT/EP/2006/062554-PCT/EP2009/066383 - PCT/EP/2011/062179 Patent application. Priority date May 05, 2005.
14. Verbeke KA, Vanbilloen HP, de Roo MJ, et al. Technetium-99m mercaptoalbumin as a potential substitute or technetium-99m labelled red blood cells. *Eur J Nucl Med*. 1993;20:473–482.
15. Kiselev MA, Gryzunov IA, Dobretsov GE, et al. Size of a human serum albumin molecule in solution. *Biofizika*. 2001;46:423–427.
16. Riesner D, Kellings K, Post K, et al. Disruption of prion rods generates 10-nm spherical particles having high a-helical content and lacking scrapie infectivity. *J Virol*. 1996;70:1714–1722.
17. Silveira JR, Raymond GJ, Hughson AG, et al. The most infectious prion protein particles. *Nature*. 2005;437:257–261.
18. Moreno NP, Tharp BZ, Erdmann DB, et al. Comparing size of microorganism. The science of microbes. Baylor Colleges of Medicine, Houston, Texas. 2008. Available at: http://www.bioedonline.org/resources/files/Microbes06.pdf. Accessed December 21, 2010.
19. Schulz HN, Jørgensen BB. Big bacteria. *Annu Rev Microbiol*. 2001;55:105–137.

World Journal of Methodology

Online Submissions: http://www.wjgnet.com/esps/
bpgoffice@wjgnet.com
doi:10.5662/wjm.v3.i4.45

World J Methodol 2013 December 26; 3(4): 45-64
ISSN 2222-0682 (online)

MINIREVIEWS

An overview of translational (radio)pharmaceutical research related to certain oncological and non-oncological applications

Marlein Miranda Cona, Peter de Witte, Alfons Verbruggen, Yicheng Ni

Marlein Miranda Cona, Yicheng Ni, Department of Imaging and Pathology, Faculty of Medicine, Biomedical Sciences Group, KU Leuven, B-3000 Leuven, Belgium
Marlein Miranda Cona, Yicheng Ni, Molecular Small Animal Imaging Centre/MoSAIC, Faculty of Medicine, Biomedical Sciences Group, KU Leuven, B-3000 Leuven, Belgium
Peter de Witte, Alfons Verbruggen, Faculty of Pharmaceutical Sciences, Biomedical Sciences Group, KU Leuven, B-3000 Leuven, Belgium
Author contributions: Miranda Cona M and Ni Y contributed equally in writing the article and in reviewing the literature; Miranda Cona M, de Witte P, Verbruggen A and Ni Y participated in the revision for important intellectual content; Miranda Cona M, de Witte P, Verbruggen A and Ni Y approved the final version of submitted manuscript.
Supported by The KU Leuven Molecular Small Animal Imaging Center MoSAIC (KUL EF/05/08) and the center of excellence *in vivo* molecular imaging research; KU Leuven projects IOF-HB/08/009 and IOF-HB/12/018; the European Union (Asia-Link CfP 2006-EuropeAid/123738/C/ACT/Multi-Proposal No. 128-498/111); the National Natural Science Foundation of China, No. 81071828; and the Jiangsu Provincial Natural Science Foundation, No. BK2010594
Correspondence to: Yicheng Ni, MD, Professor of Medicine, PhD, Chief of Theragnostic Lab, Radiology Section, Department of Imaging and Pathology, University Hospitals, KU Leuven, Herestraat 49, B-3000 Leuven,
Belgium. yicheng.ni@med.kuleuven.be
Telephone: +32-16-330165 Fax: +32-16-343765
Received: September 4, 2013 Revised: October 3, 2013
Accepted: October 18, 2013
Published online: December 26, 2013

Abstract

Translational medicine pursues the conversion of scientific discovery into human health improvement. It aims to establish strategies for diagnosis and treatment of diseases. Cancer treatment is difficult. Radiopharmaceutical research has played an important role in multiple disciplines, particularly in translational oncology. Based on the natural phenomenon of necrosis avidity, OncoCiDia has emerged as a novel generic approach for treating solid malignancies. Under this systemic dual targeting strategy, a vascular disrupting agent first selectively causes massive tumor necrosis that is followed by iodine-131 labeled-hypericin (^{123}I-Hyp), a necrosis-avid compound that kills the residual cancer cells by crossfire effect of beta radiation. In this review, by emphasizing the potential clinical applicability of OncoCiDia, we summarize our research activities including optimization of radioiodinated hypericin Hyp preparations and recent studies on the biodistribution, dosimetry, pharmacokinetic and, chemical and radiochemical toxicities of the preparations. Myocardial infarction is a global health problem. Although cardiac scintigraphy using radioactive perfusion tracers is used in the assessment of myocardial viability, searching for diagnostic imaging agents with authentic necrosis avidity is pursued. Therefore, a comparative study on the biological profiles of the necrosis avid ^{123}I-Hyp and the commercially available ^{99m}Tc-Sestamibi was conducted and the results are demonstrated. Cholelithiasis or gallstone disease may cause gallbladder inflammation, infection and other severe complications. While studying the mechanisms underlying the necrosis avidity of Hyp and derivatives, their naturally occurring fluorophore property was exploited for targeting cholesterol as a main component of gallstones. The usefulness of Hyp as an optical imaging agent for cholelithiasis was studied and the results are presented. Multiple uses of automatic contrast injectors may reduce costs and save resources. However, cross-contaminations with blood-borne pathogens of infectious diseases may occur. We developed a radioactive method for safety evaluation of a new replaceable patient-delivery system. By mimicking pathogens with a radiotracer, we assessed the feasibility of using the system repeatedly without septic risks. This overview is deemed to be interesting to those involved

in the related fields for translational research.

Key words: Translational medical research; Cancer treatment; OncoCiDia; Vascular disrupting agent; Hypericin; Myocardial infarction; Gallstone; Transflux

Core tip: Translational medicine converts scientific discovery into clinical applications. Radiopharmacy has played a multidisciplinary role. Based on unique necrosis avidity, OncoCiDia presents a generic approach for management of cancers, on which recent results on its optimization are summarized. Myocardial infarction is a clinical problem. A comparative study between infarct avid iodine-131 labeled-hypericin and commercial ^{99m}Tc-Sestamibi is presented. Cholelithiasis may cause biliary complications. The usefulness of Hyp as an optical imaging agent for cholelithiasis is demonstrated. Multiple uses of automatic contrast injectors may reduce costs but can cause cross-contaminations. We developed a radioactive method for safety evaluation of a new replaceable patient-delivery system.

Miranda Cona M, de Witte P, Verbruggen A, Ni Y. An overview of translational (radio)pharmaceutical research related to certain oncological and non-oncological applications. *World J Methodol* 2013; 3(4): 45-64 Available from: URL: http://www.wjgnet.com/2222-0682/full/v3/i4/45.htm DOI: http://dx.doi.org/10.4329/wjm.v3.i4.45

INTRODUCTION

Translational medicine refers to the creativity of joining knowledge from "bench to bedside" or from laboratory experiments to clinical trials for producing new drugs, devices, diagnostic and therapeutic options for patients. Hence, translational research is identified as a crucial interface between basic science and clinical medicine. It intends to discover better ways to solve real practical problems enhancing human health and well-being. Another current trend in translational medical research is to hybrid diagnosis and therapy into a combined approach as newly termed a "theragnostic" modality.

In the area of cancer therapeutics, transforming basic research results into clinical practice is becoming increasingly important. Cancer is one of the leading causes of mortality worldwide and little progress has been achieved in treating most of the solid tumors, which could be resistant to common therapies. Based on necrosis-avidity, OncoCiDia is a generic and unconventional theragnostic strategy recently introduced as a complementary modality to improve cancer treatability[1,2]. Unlike other cancer therapies directly attacking multimutant and refractory cancer cells, OncoCiDia may selectively treat solid malignancies by massively necrotizing the tumors plus radioactively cleansing their microenvironments, meanwhile the tumors under treatment can be visualized by nuclear scintigraphy. Thus, a dedicated acronym OncoCiDia is created to portray this cancer (Onco) management approach with both tumoricidal (Ci) and diagnostic (Dia) effects. It consists of two sequential complementary treatments involving the intravenous application of a vascular disrupting agent (VDA) followed by systemic targeted radiotherapy (STR) using a potent necrosis-avid compound iodine-131 labeled-monoiodohypericin (^{131}I-Hyp). Furthermore, to make this novel anticancer strategy clinically applicable, optimizations of the procedures for labeling, purification and formulation of the radioiodinated hypericin (Hyp) have been performed and the outcomes are summarized and commented in this overview article. Results on biodistribution, dosimetry, pharmacokinetic and, chemical and radiochemical toxicities of OncoCiDia have been also presented, which hopefully may boost the advance of this strategy into the clinic.

Myocardial infarction constitutes a health problem with large morbidity, mortality and economic burden[3]. Nuclear imaging based on myocardial perfusion tracers, which distribute in proportion to the regional myocardial blood flow, has played an important role in the assessment of tissue viability[4,5]. However, the development of diagnostic imaging agents with authentic specific avidity for necrosis has been a desired goal due to the numerous utilities they may offer. In earlier studies, the necrosis avid ^{123}I-Hyp has shown its potential usefulness as a diagnostic cardiac agent due to its notable uptake in necrotic tissues[6,7]. In a more recent experiment, its biodistribution and targetability have been compared to those of the commercially available myocardial perfusion tracer ^{99m}Tc-Sestamibi and the results have been herein summarized.

Cholelithiasis is the medical term for gallstone disease. Gallstones are hard, rock-like collections, mainly from cholesterol and bile salts that build up in the gallbladder or bile duct. Eventually, they can cause gallbladder inflammation resulting in pain, jaundice, infection and other serious complications. Because the high affinity between cholesterol and the naturally occurring fluorophore hypericin has been reported[8,9], a preliminary *in vitro* study for assessing the potential suitability of Hyp as an optical diagnostic imaging agent in patients with gallstones was performed and the results are presented in this work.

Multiple uses of automatic contrast injection systems during imaging procedures can reduce costs and save resources. However potential outbreak associated with cross-contaminations with blood-borne pathogens of infectious diseases through the contrast medium may occur. The Transflux contrast delivery system is a simple tube delimited by two one-way valves intended to deliver contrast media from a reservoir to the patient and with the need to only change the tubing in direct contact with the patient blood. It incorporates a safety zone and a one-way valve in the patient line that allow the delivery system and the vein to be flushed and the blood reflux to be prevented. By mimicking microbial pathogens

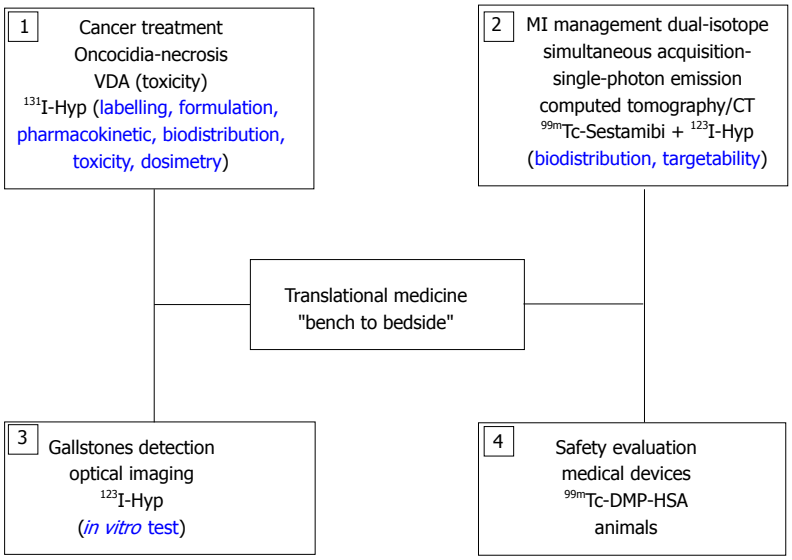

Figure 1 Schematic structure of the translational research activities covered by the overview article. ^{99m}Tc-sestamibi: Technetium-99m labeled-hexakis (2-methoxyisobutylisonitrile); ^{99m}TcDMP-HSA: Technetium-99m dimercaptopropionyl human serum albumin; $^{123/131}$I-Hyp: Iodine-123/iodine-131 labeled monoiodohypericin; MI: Myocardial infarction; VDA: Vascular disrupting agent.

with a particulate radiotracer, we developed a radioactive method for quantitative safety evaluation of this new replaceable patient-delivery system and the main findings are reported here.

This overview paper is in the framework of the full 4-year doctoral training, in which translational research has been attempted as a key component for resolving important problems in diverse medical fields (Figure 1).

APPLICATION OF TRANSLATIONAL RESEARCH IN THERAGNOSTIC ONCOLOGY

Background

Cancer is a complex group of malignant diseases influenced by genetic and environmental factors. Over the past decades, the incidence and prevalence of cancer have raised with an overall estimation of about 20 million new cases by 2030[10]. The costs associated with cancer diagnosis, therapy, and follow-up have drastically soared. Conventional therapies including surgery, chemotherapy and external beam radiotherapy are often ineffective for treating resistant and disseminated solid malignancies. Novel and cost-effective approaches, once available, are essential to improve cancer treatability and curability.

STR is a radiotherapy that makes use of systemically administered radioactive compounds for delivering lethal radiation doses to the tumor while preserving normal tissues. Several radioactive agents have been clinically used, for instance, radioiodine for thyroid cancer owing to its specific uptake by thyroid glandular tissues[11]; iodine-131 metaiodobenzylguanidine for treating pheochromocytoma[12] and neuroblastoma[13]; Metastron (strontium-89 chloride) as a palliative treatment in patients with bone metastases[14]; and radioactive microspheres for radioembolization of liver cancer[15]. Anti-CD20 monoclonal antibody (MoAb) conjugated to I-131 (tositumomab, Bexxar®)[16] or yttrium-90 (ibritumomab tiuxetan, Zevalin®)[17] for treating non-Hodgkins lymphoma, and somatostatin derivatives labeled with bound indium-111, lutetium-177 or yttrium-90 for neuroendocrine tumors (NETs)[18,19] are lately introduced, constituting a step forward in tumor specific targeting.

However, most of the above-mentioned cancer types represent a small proportion among the overall cancer cases. Malignant solid tumors, which represent the major cancer incidence worldwide, have been difficult to treat due to their histological diversity, disorganized angiogenesis and unpredictable mutations. Once carcinogenesis is established, tumor cells become resistant to therapies due to the multiple escape mechanisms facilitated by intrinsic mutations and/or overlapping molecular pathways. Even if a proper radioactive MoAb is chosen, in most of the cases, only small amounts of injected dose (0.001%-0.1% /g) could accumulate in the tumor[20]. Low absorbed doses (1500 cGy) are subsequently reached in cancer cells that are much lower than the usually required doses (5000 cGy) for getting therapeutic responses[21,22]. With somatostatin derivatives-based radiopharmaceuticals characterized by high affinity for distinct receptors overexpressed in the tumor, short-term accumulation in the tumor and retention in normal tissues have also been reported[23]. Therefore, necrosis as a generic alternative target has been utilized for potential theragnostic applications (Figure 2).

Tumor necrosis treatment

Rather than hitting cancer cells undergoing numerous mutations[24,25] that cause uncontrollable growth and escape from annihilation, leading to post-therapeutic cancer resistant clones[24], an innovative anticancer approach called tumor necrosis treatment (TNT) was introduced[26,27]. Since the proportion of dead tissue in fast-growing tumors can be more than 50% of the total cancer volume due to tumor vascular deformation or insufficient blood supply[28,29], necrosis could become a generic target in almost all solid tumors. TNT approach uses radiolabeled MoAbs that spare normal tissue and target naturally occurring intracellular antigens (a complex of double-stranded DNA and histone H1-antigens)

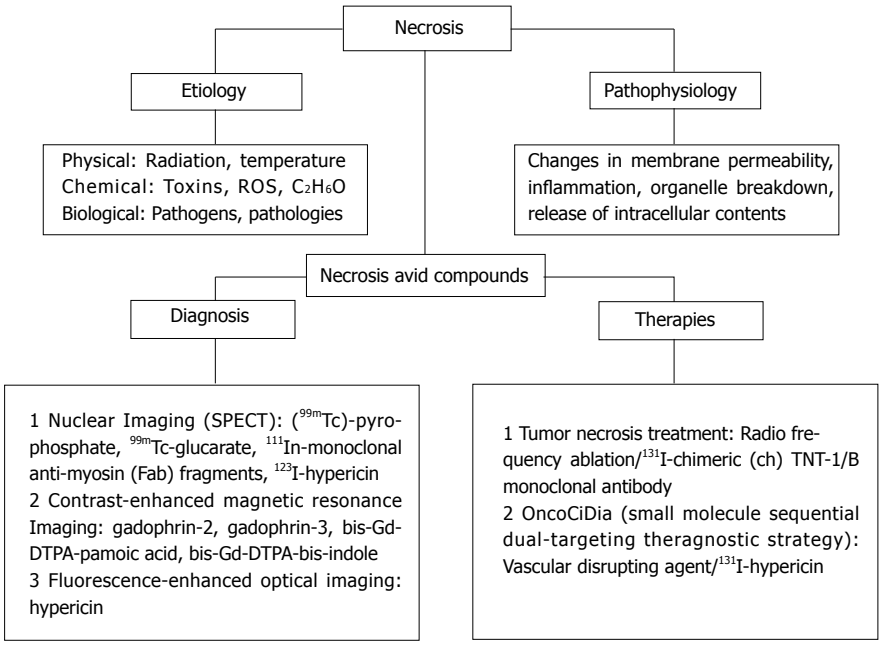

Figure 2 Flow diagram of the included research topics. ^{99m}Tc: Technetium-99m; ^{111}In: indium-111; ^{123}I: Iodine-123; ^{131}I: Iodine-131; C_2H_6O: Ethanol; DTPA: Diethylene triamine pentaacetic acid; Fab: Antigen-binding fragment; Gd: Gadolinium; ROS: Reactive oxygen species; SPECT: Single photon emission computed tomography; TNT: Tumor necrosis treatment.

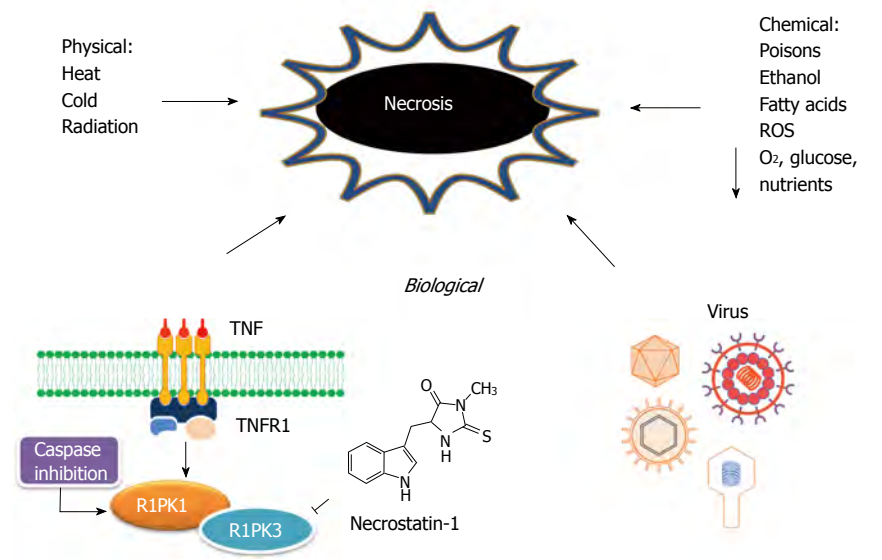

Figure 3 Schematic representation of the etiology of necrosis. ROS: Reactive oxygen species; TNT: Tumor necrosis treatment; RIPK1/3: Receptor-interacting protein kinase 1 and 3; TNFR1: Tumor-necrosis factor receptors 1.

present throughout tumor necrosis[30,31]. Unlike conventional STR, it is a crossfire-dose therapeutic modality, in which the radiation dose deposited to cancer cells only comes from radionuclides on surrounding necrosis.

Definition, etiology and pathophysiology of necrosis: The term of necrosis is originated from the Greek prefix "necros", meaning "dead". It constitutes an irreversible process or "no return" status in the cell life[32]. Cell death by necrosis has been historically stereotyped as an unregulated process[33]. Any severe lesions caused by physical stresses, toxins, infections or genetically programmed injuries if reaching a certain degree and receiving no intervention may alter physiological homeostasis, eventually leading to tissue or organ necrosis[34]. However, it turns increasingly evident that the multi-pathway cell-death program apoptosis may not be the only cellular mechanism involved in regulating cell death[35]. Programmed necrosis or necroptosis has emerged as a specialized biochemical mechanism that can be induced by different stimuli such as tumor-necrosis factor receptors (TNFR1, TNFR2)[36], inactivation of cysteine-aspartic acid proteases (caspase)[37] and caspase-8 mutations[38]. It becomes clear that necroptosis could be regulated by the kinase receptor-interacting protein 1 (RIPK1), which constitutes the molecular target of necrostatins, an emerging class of cytoprotective drugs inhibiting specifically necroptotic cells[37]. Recently, the kinase activity of RIPK3, a family member of RIPK1, has also been related to programmed necrosis[39] (Figure 3).

Necrosis is commonly believed to be a passive process since it involves no protein production, is not restrained by any homeostatic mechanisms, and includes almost negligible energy requirements. The necrotic cells can no longer retain the integrity of the cell or cytoorganelle membranes and perform inherent functions. Af-

ter losing the ability to maintain homeostasis, biological fluids from the blood cross the damaged cell membrane and enter the intracellular space, leading to organelles enlargement, production of toxins and activating enzymes associated to the degradation of cellular life molecules. The swollen organelles become nonfunctional, ceasing the synthesis of proteins and ATP. The mitochondrial swelling causes cytolysis and the debris is discharged into the surroundings, which triggers tissue inflammation regulated by small proteins-cytokines, reactive oxygen species and certain immune system cells[40]. The organism interprets the presence of the debris as signal of tissue injury and reacts to defend itself. In response, immune system cells migrate into the site of damage and combat the supposed invading microorganisms[40]. Dissociation of ribosomes from the endoplasmic reticulum and nucleus disintegration with chromatin condensation take place in turn[41]. The dead cells eventually fade away because of the combination of enzymatic denaturation and fragmentation process, followed by polymorphonuclear leukocyte phagocytosis of solid particles[42].

Preclinical studies and clinical trials on TNT: In a pioneer pre-clinical study conducted on a ME-180 human cervical carcinoma model with ^{131}I-labeled TNT-1 MoAb, Chen *et al*[31] proved the effective and preferential targeting of this radiotherapeutics within the tumor, which established the potential clinical usefulness of TNT. To date, about 200 patients have been treated with TNT worldwide. A phase I study of ^{131}I-chimeric(ch) TNT-1/B MoAb for the treatment of advanced colon cancer was performed. The infusion of ^{131}I-chTNT-1/B MoAb was well tolerated and showed no significant non-hematologic effects. Based on tumor cross-product response criteria, however, none of the patients exhibited complete or partial response[43]. Phase I and Ⅱ trials of convection-enhanced delivery of ^{131}I-chTNT-1/B MoAb were conducted on patients with high-grade adult gliomas, showing promising therapeutic outcomes[44]. Similar results were found in a pivotal study in patients with advanced lung cancer treated with ^{131}I-chTNT-1/B MoAB[45]. More recently, genetically engineered Fab' and F(ab') 2 constructs of chimeric TNT (chTNT)-3 antibody labeled with indium-111 were prepared and preclinically evaluated. The conjugates showed faster body clearance, better biodistribution but lower tumor uptake than the parental ^{111}In-labeled chTNT-3 in tumor-bearing mice[46].

To increase the amount of MoAb binding-necrotic sites in the tumor, necrosis-inducing treatments (NITs) such as radiofrequency ablation were also used as starting complementary techniques[47].

However, myelosuppression due to unfavorable pharmacokinetic properties of MoAbs constitutes an important dose limiting factor that prevents substantial improvement of TNT-based modality[43,44].

OncoCiDia

OncoCiDia, also known as small molecule sequential dual-targeting theragnostic strategy[1], is a novel anticancer approach with great potential for treating solid tumors. Relying on a soil-to-seeds concept, it offers a one-stop-shop for diagnostic imaging, treatment and follow-up[2]. Similar to the TNT approach, it is based on the natural phenomenon of necrosis. However, instead of using radioactive MoAb with large molecular size (150 kDa) and complex pharmacokinetics, it involves two small compounds (< 1 kDa) with pre-identified high and divert but complementary targetability. The intravenously (IV) administered VDA triggers selective tumor vascular shutdown and subsequent central necrosis. However, a viable rim of tumor cells in the periphery always exists as seeds for repopulation of cancer cells[48]. ^{131}I-Hyp is then IV injected, which preferentially localizes at the newly generated necrotic sites and acts as a cleansing shot to lethally irradiate residual tumor cells through a crossfire effect[2]. The small molecular size of ^{131}I-Hyp makes it possible to permeate fast through tissues and target less accessible sites throughout the solid tumor. This may overcome the initial barriers faced by the systemic delivery of MoAb, which limits diffusion from blood vessels and inhibits drug tumor penetration[21,49].

Vascular disrupting agents: Vascular disrupting agents (VDAs) are a novel category of potential anticancer drugs that induce tumor vascular shutdown by destroying the endothelium of tumor vasculature. It has been reported that blood vessels in tumors proliferate more rapidly than those in normal tissues[49]. Newly formed endothelial cells are more sensitive than mature ones that own a well-developed actin cytoskeleton and may retain the cell shape in spite of depolymerization of the tubulin cytoskeleton caused by the VDA[50]. After VDA administration, the occlusion of blood-supplying vessels and capillary sprouts obstructs oxygen and nutrient supply to the tumor cells, compromising cellular integrity and eventually leading to hemorrhagic tumor necrosis[51]. Different groups of VDAs have been developed, *e.g.,* tubulin-binding agents cause microtubule depolymerization by binding either the colchicine or vinblastine sites, whereas flavonoid derivatives selectively obstruct tumor-related vessels due to their indirect pharmacodynamic effects[51]. VDAs can be obtained from nature such as combretastatins (CA4P, OXi-4503, and AVE-8062), colchicines (ZD6126) and phenylahistin (NPI-2358), whilst others are synthetic compounds (DMXAA, MN-029 and EPC2407)[51].

Hyp: Hyp is a red-colored anthraquinone derivative (naphthodianthrone), which is one of the principal active compounds of the genus Hyp (Clusiaceae) comprising roughly 450 species worldwide[52]. Hyp was initially found in the dark glands of the flowering parts from Hyp perforatum L (St. John's Wort)[53], an aromatic, perennial plant. Hyp can be also obtained from fungi Dermocybe[54] or from endophytic fungi growing in different plant species[52]. However, the most commercially available Hyp

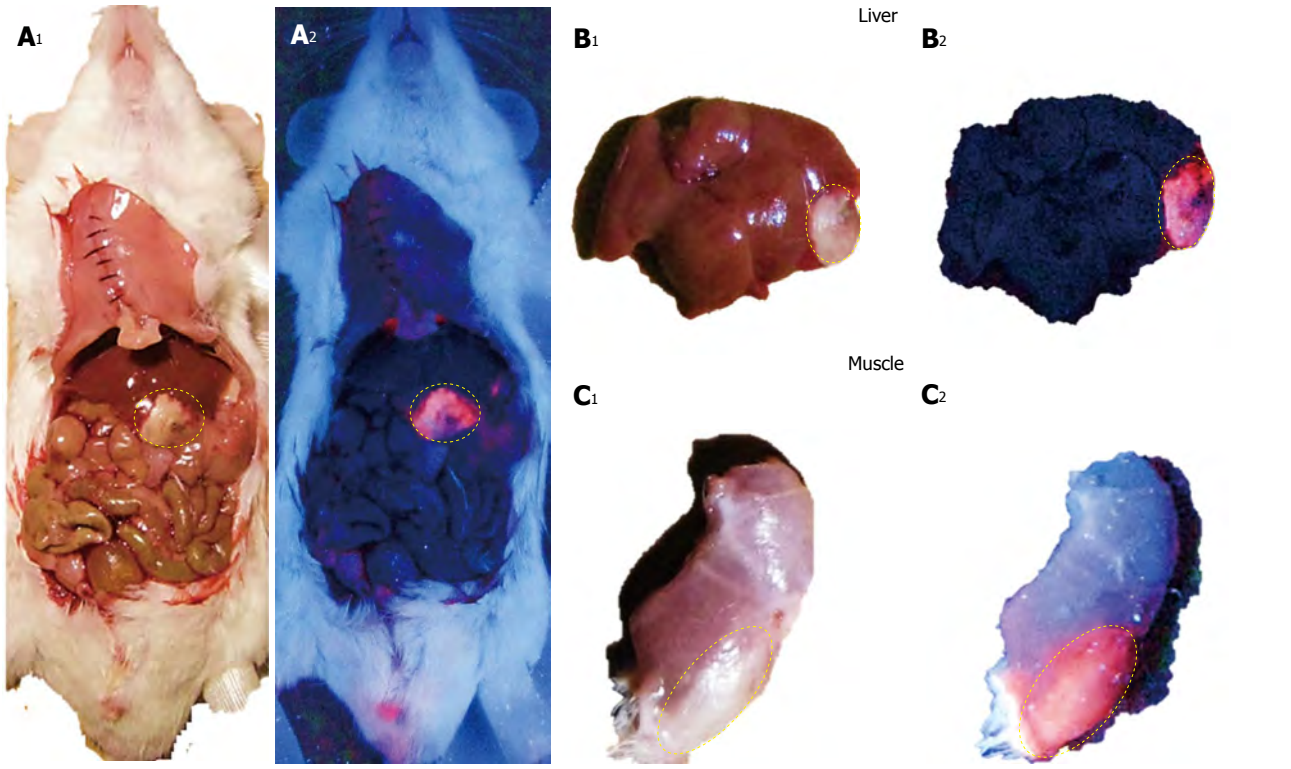

Figure 4 Macroscopic digital imaging of a mouse with acute ethanol-induced necrosis in the liver and muscle having received 5.0 mg/kg hypericin in DMSO/PEG400/water (25:60:15, v/v/v). Under normal tungsten light, viable liver, intestines and muscle show normal appearances whereas hepatic infarction and muscle necrosis appear as white cheesy tissue (A_1, B_1, C_1). With a UV light of 254 nm, a bright red fluorescence from liver (A_2, B_2) and muscle necrosis (C_2) but a lack of fluorescent signal from the liver (A_2, B_2), viable muscle (C_2) and other abdominal structures were observed (A_2). DMSO: Dimethyl sulfoxide; PEG400: Polyethylene glycol 400; UV: Ultraviolet.

compounds are synthesized.

Hyp has been considered a vinylogous carboxylic acid. Its deprotonations are likely at the phenolic hydroxyl groups at the peri- and bay-regions having different acidities. In aqueous system the bay- and peri-regions show estimated pKa values of 1.7 and 12.5[55], respectively. Hyp showed a non-planar conformation owing to the repelling interactions among the side chains of the aromatic skeleton[56]. The proximity of acidic and basic functional groups allows the formation of intramolecular hydrogen bonds, which influence the tautomeric equilibria and acid-base properties[55]. Hyp has 16 conceivable tautomers[57]. Among them, the most stable is the 7, 14-dioxoisomer[58]. Hyp dissolves in polar solvents over concentrations of 10^{-3} mol/L, producing red fluorescent solutions. It is soluble in Dimethyl sulfoxide (DMSO), ethanol, pyridine, methanol, acetone, butanone, ethyl acetate and aqueous alkaline solutions[59]. It has been found in soluble form under physiological conditions due to the complex formation with biological macromolecules, mainly low-density lipoprotein (LDL)[60].

Hyp is a natural product of pharmaceutical interest due to its ever-expanding anti-inflammatory[61], antiretroviral[62], antimicrobial[63], antitumor[64] and antidepressive[65] activities. Recently, it has been found with a highly selective affinity for necrosis[6,7] (Figure 4).

The mechanisms associated with the necrosis avidity of Hyp remain unknown and a number of hypotheses have been proposed. Hyp specifically accumulates in exposed sites of degraded life molecules in the necrotic cell debris[66]. Binding to LDL[60] and serum or interstitial albumins[67] have been put forward as potential interaction pathways. Hyp has also been found to show highly selective avidity for lipid components including cholesterol[8], phosphatidylserine and phosphatidylethanolamine[68] present in the cell membrane bilayer.

Iodine isotopes: Iodine-123 (^{123}I) is a halogen with a physical half-life of 13.1 h. It decays by electron capture to tellurium-123, emitting gamma radiation with a main energy of 159 kEV, which is exploitable for nuclear scintigraphy, biodistribution and radiodosimetry studies.

Iodine-131 (^{131}I) with a decay half-life of 8.02 d is the most common iodine radioisotope utilized in medical applications owing to its relatively easy availability and low cost. It decays by emission of beta minus electrons with a maximal energy of 606 kEV (89% abundance) and a tissue penetration of 0.6-2.0 mm[69] as well as 364 kEV gamma rays of 81% abundance. ^{131}I destroys tissue by short-range beta radiation, causing DNA damage and cell death to the cell that takes up the tracer by self-dose effect and to other cells up to several micrometers away by cross-fire effect.

Due to radioprotection reasons, ^{123}I is frequently used

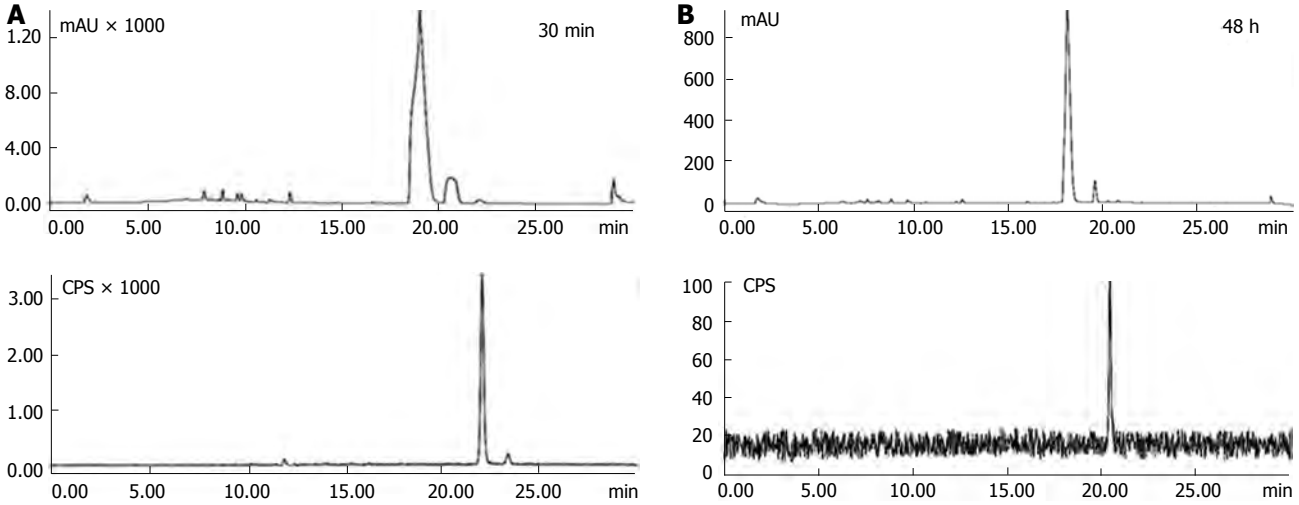

Figure 5 High performance liquid chromatographic analysis of the non-purified iodine-123 labeled hypericin with Ultraviolet (254 nm) and radiometric detection. A: Ultraviolet-chromatogram of the starting reagent hypericin (Hyp) with a retention time of 19.18 min (upper part) and radiochromatogram (lower part) of ^{123}I-Hyp eluting at 22.13 min with a mean radiochemical yield of 95.4%; B: High performance liquid chromatographic analysis of the non-purified ^{123}I-Hyp at 48 h after labeling. A single narrow peak coming out at 21.90 min (lower part) suggests the *in vitro* stability of ^{123}I-Hyp over time. CPS: Count per second.

as surrogate of ^{131}I for labeling optimization, biodistribution and dosimetry studies with the mutually interpretable outcomes.

Preparation of $^{123/131}$I -labeled-monoiodohypericin: Radioiodination *via* direct electrophilic substitution is a simple method based on *in situ* formation of positively charged iodine (I^+) using mild oxidants such as *N*-chloro para-toluenesulfonylamide (chloramine T), peracetic acid and 1,3,4,6-tetrachloro-3α, 6α-diphenyl glycoluril (Iodogen). The radioactive iodine atom in an oxidized form replaces a hydrogen atom of an activated aromatic ring. Since Hyp is a polycyclic aromatic quinone having hydroxyl substituents, it can be efficiently radioiodinated.

Two main methods for direct radiolabelling of Hyp with iodine isotopes have been described. Bormans *et al*[70] reported a radioiodination procedure of Hyp in ethanol using phosphoric acid and peracetic acid as oxidant for 30 min. On high performance liquid chromatography (HPLC), radiochemical yields ranging between 70%-97% were achieved[70]. Sun *et al*[71] described a simple method, in which Hyp in DMSO is labeled with $^{131/123}$I using iodogen as oxidant (either in a pre-coated tube or in powder form), at pH value between 6.5-7.5 for 2 to 10 min. Labeling yields higher than 99% were attained as indicated by paper chromatography (PC).

However, although PC is useful for the purpose of identification due to its convenience and simplicity, we investigated the method developed by Sun and Ni using HPLC. This technique provides high resolution and allows identifying and quantifying small amounts of substances. Labeling conditions were screened for varying reaction parameters such as Hyp mass, Hyp/iodogen molar ratio and reaction time. Stability over time of the radioactive Hyp was also checked. For radiochemical yield determination and purification, the effect of different mobile phases either in gradient or isocratic modes was studied on a quaternary HPLC system equipped with a Ultraviolet (UV) absorbance (254 nm) and radiometric detector. An XTerra® C18 column (4.6 mm × 150 mm, 5.0 μm) and a flow rate of 1.0 mL/min were used for radiochemical yield analysis. On the other hand, an XTerra® C18 semi-preparative column (10 mm × 250 mm, 10 μm) and a flow rate of 3.0 mL/min were set for purification. The peak areas of Hyp and radioiodinated Hyp were considered as response variables in this optimization test.

The preferred conditions for Hyp radioiodination were 2.0 mg Hyp in a molar ratio (Hyp: iodogen) of (3.4:1); 90/10, mL/L DMSO/50 mmol/L sodium phosphate buffer at pH 7.4 for 20 min. For radiochemical yield determination, a mobile phase consisting of acetonitrile/5 mmol/L ammonium acetate buffer pH 7.0 in gradient mode (0 min: 5:95 v/v, 25 min: 95:5 v/v, 30 min: 5:95 v/v) provided the best resolution between adjacent peaks. UV/radio-chromatograms showed unlabeled Hyp and iodine-123-labeled monoiodohypericin (^{123}I-Hyp) with t_R of 19.18 ± 0.15 min and 22.13 ± 0.05 min, respectively. Free iodide was not observed (Figure 5A). ^{123}I-Hyp was prepared with specific activity above 50 GBq/μmol in a radiochemical yield of 95.4% and remained stable over 48 h at room temperature (Figure 5B). As confirmed by mass spectrometry, the small differences between the labeling yield obtained by PC and HPLC were due to the concurrent formation of di-[(^{123}I) iodohypericin in low percentage (approximately 3%), which was detected together with mono-(^{123}I)] iodohypericin by PC.

After labeling, excessive reagents (unlabeled Hyp and iodogen) were removed by HPLC using acetonitrile/5 mmol/L ammonium acetate buffer at pH 7.0 as mobile phase in a gradient mode (0 min: 75:25, v/v, 5 min: 75:25, v/v, 30 min: 90:10, v/v). Good separation between Hyp

and radioiodinated Hyp peaks was achieved. ^{123}I-Hyp was obtained with a radiochemical purity above 99.0%. However, broad peaks with long retention times for Hyp and radioiodinated Hyp were typically observed during the purification process. It seems once radioiodinated Hyp is mixed with unlabeled Hyp in a total mass of about 2 mg, they might undergo partial retention in the HPLC system due to aggregate formation. Under physiological conditions, such aggregates may show reduced necrosis affinity and increased uptake in organs of the mononuclear phagocyte system (MPS), hampering the potential clinical usefulness of ^{131}I-Hyp for OncoCiDia.

Confronted problems: OncoCiDia has shown the best results using a mixture of radioiodinated Hyp/unlabeled Hyp[1]. To overcome the limitations related to the purification process, we recommended the clinical use of the non-purified radioiodinated Hyp, which is attained with high labeling yields (> 95%). However, conditions for Hyp radioiodination require excess of starting material at high concentrations of DMSO, which also dissolved the oxidizing agent iodogen. As a result, both reagents remain in the formulation of the non-HPLC purified radioiodinated Hyp, giving toxicity concerns. Moreover, the unlabeled Hyp present in the mixture is in a concentration range of 10^{-3} mol/L, in which it may aggregate in biocompatible aqueous formulations. Regarding $^{123/131}$I-Hyp, the incorporation of an iodine atom into a molecule can also result in a more lipophilic and less water soluble derivative[72]. Under these circumstances, a proper delivery system is essential for preventing aggregate formation and subsequently ensuring efficient targeting to necrotic tumor. Another potential issue arises with the co-injection of unlabeled Hyp which could influence $^{123/131}$I-Hyp on the biodistribution and targetability over time. Since the treatment of solid tumors requires the preferential delivery of a radiotherapeutic dose to the tumor while preventing normal tissues from undesired side effects[73], the dosimetry of this co-injection approach has to be estimated, as well. These above-mentioned problems have been assessed or addressed below.

Formulation: For $^{123/131}$I-Hyp/Hyp, the co-solvency approach seems to be a good alternative due to its rapidness and simplicity. In preclinical investigations, a formulation consisting of water/ polyethylene glycol (PEG 400) (80/20, v/v) has been reported[1]. Pure DMSO as solvent for the poorly water soluble $^{123/131}$I-Hyp/Hyp has also been used[74]. However, further optimizations are needed.

In a recent study, we tested several delivery systems for $^{123/131}$I-Hyp/Hyp using macroscopic and microscopic techniques and the results are summarized in Table 1[75]. Overall, formulations with a water content below 40% showed red fluorescent solutions without aggregate formation. In contrast, formulations containing around 70% water appeared as cloudy brownish solutions with reduced fluorescent properties. Animal studies confirmed the previous *in vitro* observations. For instance, when DMSO/PEG 400/water (25:60:15, v/v/v) was used as a vehicle, $^{123/131}$I-Hyp/Hyp showed low uptake in MPS organs, high necrosis affinity and striking tumoricidal effects days after OncoCiDia application. With $^{123/131}$I-Hyp/Hyp in DMSO/saline (20:80, v/v), instead, radioactivity accumulation in MPS organs but low uptake in necrotic tumor were found. Consequently, poor radiation dose was deposited in the tumor, leading to disease progression because of rapid repopulation of residual cancer cells at the tumor periphery after VDA attack[75].

However, earlier studies have reported that the common pharmaceutical solvents may have biological and pharmacological activity mainly when given undiluted[76-78]. Alternatively, the water-soluble sodium cholate (NaCh), a naturally occurring liver-produced surfactant with low toxicity, was assessed as a potential solubilizing agent for ^{123}I-Hyp/Hyp in an animal model of acute myocardial infarction (MI) (Cona *et al*[79]). The amphiphilic NaCh molecule with hydrophilic and hydrophobic sides of different solubility properties forms micelles, which act as emulsifier above the critical micellar concentration. Necrosis avidity of ^{123}I-Hyp/Hyp dissolved in a NaCh solution and its favorable biodistribution were demonstrated (Figure 6). The suitability of NaCh as a solubilizing agent of ^{123}I-Hyp for hotspot imaging of acute MI could be demonstrated (Cona *et al*[79]).

Biodistribution and dosimetry studies: Tissue distribution of ^{123}I-Hyp/Hyp was studied on animal models either of reperfused partial liver infarction (RPLI)[80] or ethanol-induced muscle necrosis. Dosimetric extrapolations of ^{131}I-Hyp from animals to humans were attempted using biodistribution data of ^{123}I-Hyp in RPLI animals in combination with Organ Level Internal Dose Assessment/Exponential Modeling software, microsphere model and human phantoms of both genders.

^{123}I-Hyp was accumulated at high concentrations in hepatic infarction and muscle necrosis but low uptake either in viable liver or muscle was detected (Figure 7), as previously reported[1,7,74,75]. Dosimetry studies revealed much higher (> 100 times) absorbed doses of ^{131}I-Hyp in hepatic infarction than in normal liver (Cona *et al*[79]). Based on this finding, such doses seem to be much higher than those estimated with other radiotherapeutics under investigation or currently used in clinic (Table 2)[31,81-88]. This corroborates the high affinity for tumor necrosis as well as the tumor shrinkage and growth delay previously observed in animals bearing different engrafts tumors after a single treatment with OncoCiDia (Figure 8)[1,75,89].

In biodistribution studies, ^{123}I-Hyp was cleared within 24 h with reduced blood pool radioactivity. Thyroid, the dose limiting organ for ^{131}I-labeled products, showed almost no radioactivity concentration due to the absence free iodide at earlier time points, suggesting *in vivo* stability of $^{123/131}$I-Hyp. However, an increased uptake in the gland was detected, starting at the second day after tracer administration. In the lungs, a persistent ^{123}I-Hyp uptake was found, leading to a moderately absorbed radiation

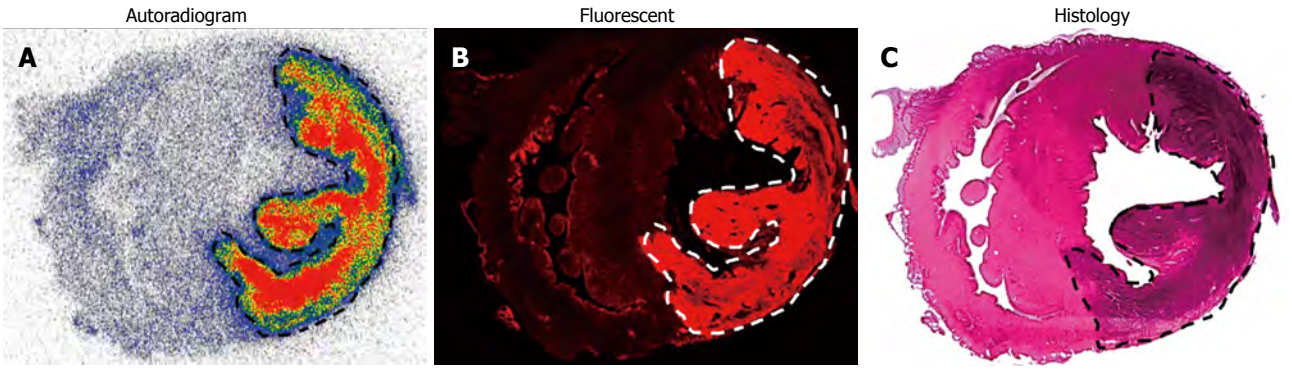

Figure 6 Post-mortem analysis of infarcts and viable heart tissues from rabbits with acute reperfused myocardial infarction having intravenously received iodine-123 labeled hypericin/hypericin dissolved in a 0.07 mol/L solution of the liver-produced surfactant sodium cholate. A: A typical autoradiogram of 50-μm-thick sections reveals higher tracer uptake in infarction than in viable myocardium. The color code bar indicates the coding scheme for the radioactivity; B: Microscopic images of 50-μm-thick sections confirm the selective affinity of the highly fluorescent iodine-123-labeled-hypericin/hypericin for acute myocardial infarction in contrast to the low fluorescent signal found in viable myocardium; C: The H and E-stained section corroborates the location of the viable myocardium tissue and the presence of myocardial necrosis characterized by scattered hemorrhage.

Table 1 Evaluation of physical properties of different formulations of ^{123}Hyp/Hyp examined by macroscopic digital imaging under white light and ultraviolet light (254 nm) and by microscopy over a corresponding drop in bright field and fluorescence illumination mode

Formulation	Macroscopic digital imaging	Microscopy
DMSO/saline (20/80, v/v)	Cloudy brownish solution, no fluorescence	Massive formation of aggregates reduced fluorescent intensity
DMSO/water (25/75, v/v)	Cloudy brownish solution, no fluorescence	Massive formation of aggregate reduced fluorescent intensity
DMSO/D10W (25/75, v/v)	Cloudy brownish solution, no fluorescence	Massive formation of aggregates reduced fluorescent intensity
DMSO/D20W (25/75, v/v)	Cloudy brownish solution, no fluorescence	Massive formation of aggregates reduced fluorescent intensity
DMSO/serum (25/75, v/v)	Cloudy brownish solution, moderate fluorescence signal	Massive formation of aggregates moderate fluorescent intensity
DMSO/PEG 400/water (25/60/15, v/v/v)	Bright red solution, highly fluorescent	No aggregates formation; strong, homogeneous fluorescence
EtOH/PEG 400/water (10/50/40, v/v/v)	Dark red solution, moderate fluorescence	Aggregate formation; moderate, heterogeneous fluorescence,
EtOH/PEG 400/water (10/60/30, v/v/v)	Red solution, minimum aggregation, high fluorescence	Some aggregates; strong, homogeneous fluorescence
PEG 400/water (60/40, v/v)	Red solution, high fluorescence	Some aggregates; strong, homogeneous fluorescence
PEG 400/water (70/30, v/v)	Bright red solution, highly fluorescent	Some aggregates; strong, homogeneous fluorescence
PVP-10000	Dark red solution, moderate fluorescence	Aggregate formation; reduced fluorescence intensity
PVP-29000	Dark red solution, moderate fluorescence	Aggregate formation; reduced fluorescence intensity
β-Cyclodextrins	Cloudy brownish solution, no fluorescence	Massive formation of aggregates reduced fluorescent intensity

DMSO: Dimethyl sulfoxide; D10W: 10% dextrose; D20W: 20% dextrose; EtOH: Ethanol; PEG 400: Polyethylene glycol 400; PVP: Polyvinylpyrrolidone.

dose of ^{131}I-Hyp. The highest levels of radioactivity were found in the intestines, which constitute the major elimination pathway of this radioactive compound. As a consequence, bowel structures received a high radiation dose, being identified as one of the dose limiting organs for OncoCiDia.

Effect of added Hyp on biodistribution and targetability of $^{123/131}$I-Hyp: In STR, it is known that the mass of the unlabelled (carrier) compound present in the final radioactive solution can be critical for high specific activities that are required for maximal radioactivity accumulation in the disease site. In a recent investigation for OncoCiDia, we proved that the co-injection of unlabelled Hyp positively affected the necrosis uptake of the radioiodinated Hyp in RPLI rats[90]. Although both preparations of ^{123}I-Hyp with micro- or Hyp-added dosing showed similar tissue distributions and major hepatobiliary excretion, it was found that the carrier-added ^{123}I-Hyp accumulated at higher concentrations in necrosis. Similarly, long retention into tumor necrosis for several weeks could characterize the carrier-added ^{131}I-Hyp (Figure 8 case 2), which explains the striking therapeutic effects observed in the previous experiments[1,75,89].

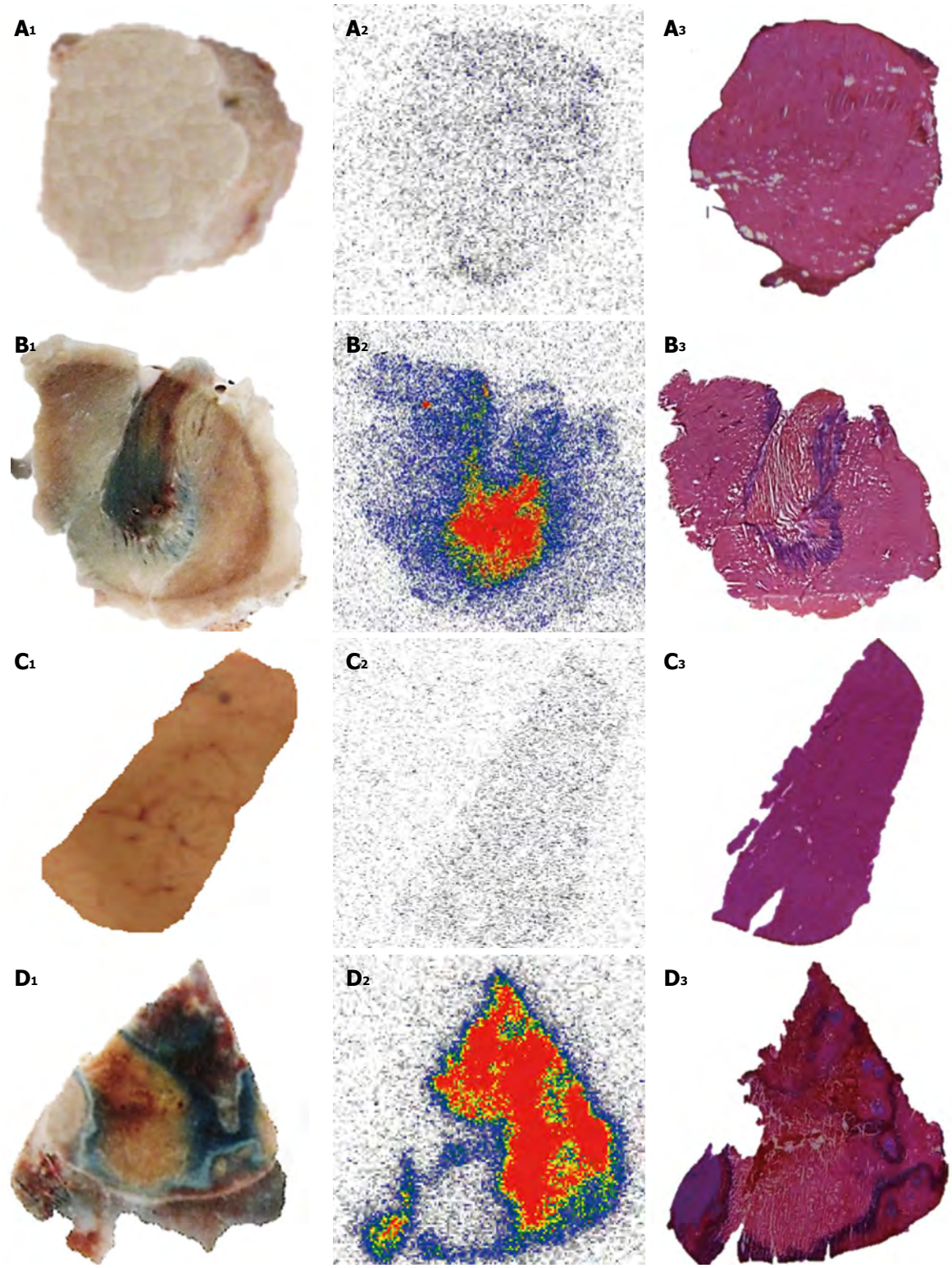

Figure 7 Post-mortem study of necrotic and viable tissues in the liver and muscle from animal models either of reperfused partial liver infarction or ethanol-induced muscle necrosis pre-injected with iodine-123 labeled hypericin/hypericin followed by 1% Evans blue solution. A, B: Muscle; C, D: Liver. The hepatic infarction (A_1) and necrotic muscle (B_1) retain Evans blue as blue hyper intense areas, with viable liver (C_1) and normal muscle (D_1) without staining. Autoradiograms of 50-μm-thick sections show high tracer uptake in hepatic infarction (A_2) and muscle necrosis (B_2) but low accumulation either in viable liver (C_2) or muscle (D_2). The color code bar represents the code for the radioactivity concentration. By histology, the presence of hepatic infarction (A_3) and muscle necrosis (B_3) and the location of the viable liver (C_3) and muscle (D_3) tissues are verified.

Toxicity studies: OncoCiDia is a two-step anticancer strategy involving different compounds with potential chemical and/or radiochemical toxicities, which have been investigated, and possible solutions are herein proposed.

Toxicity from VDAs can happen as a result of the ef-

Table 2 Dosimetry aspects of different anticancer therapeutic agents under pre-clinical and clinical investigation

Therapeutics	Dosimetry calculations	Species	Targeting tissue	Pathology	Dose to tumor (mGy/MBq)	Ref.
^{131}I-Hyp	OLINDA/EXM software	RPLI rats	Necrotic tissue	Solid tumors	276–93600	[79]
^{131}I-Labeled TNT-1 monoclonal antibody	Organ uptake-time integration by trapezoid method Whole body image analysis	Nude mice bearing ME-180 human cervical tumors	Histone fraction H1 in necrotic tissues	Cervical carcinoma cell	366–3610	[31]
^{131}I-m-iodobenzylguanidine (MIBG)	MicroPET/CT 124I-MIBG OLINDA/EXM software	Mice bearing A431 human epithelial carcinoma xenografts	Norepinephrine transporter	Neuroblastoma	97–380	[80]
^{131}I- labeled monoclonal antibody MN-14	MIRDOSE3 software	Nude mice with intraperitoneal LS174T tumors	Carcinoembryonic antigen	Peritoneal metastases of colorectal origin	-16200	[89]
^{131}I-tositumomab	SPECT/CT Imaging DPM Monte Carlo electron and photon transport program	Humans	CD20-positive B-cells	Refractory B-cell NHL	2.81 (mean)	[81]
^{177}Lu-DOTA-AE105	Organ uptake-time integration by trapezoid method Sphere model	Nude mice bearing colorectal HT-29 tumor	uPAR-positive HT-29 xenograft	Colorectal cancer	5.8	[82]
^{177}Lu-pertuzumab	Organ uptake-time integration by trapezoid method Sphere model	BALB/c (nu/nu) Mice with HER-2–overexpressing xenografts	HER-2 tyrosine kinase receptor	Breast cancer	-6900	[83]
^{186}Re-1-hydroxy- ethylidene-1,1 diphosphonic acid	MIRDOSE 3.1 software	Humans	Bone mineral metabolite	Skeletal metastases	23–34	[84]
^{90}Y-ibritumomab tiuxetan	PET/CT Imaging DPM ^{89}Zr-ibritumomab tiuxetan OLINDA/EXM software	Humans	CD20-positive B-cells	Relapsing NHL	8.6–28.6	[85]
^{90}Y- DOTA0-DPhe1-Tyr3-octreotide	SPECT/CT Imaging DPM ^{111}In-DOTA-TOC	Humans	Somatostatin receptor subtype 2	NETs	4-31 (mean 10)	[86]

CT: Computed tomography; DOTA: 1,4,7,10-tetraazacyclododecane-1,4,7,10-tetraacetic acid; ^{131}I: Iodine-131; ^{177}Lu: Lutetium-177; NETs: Neuroendocrine tumors; OLINDA/EXM: Organ level internal dose assessment/exponential modeling; PET: Positron emission tomography; ^{186}Re: Rhenium-186; RPLI: Reperfused partial liver infarction; SPECT: Single-photon emission computed tomography; TNT: Tumor necrosis treatment; DPM: Dose planning method; NHL: Non-Hodgkin lymphoma; DOTA-TOC: ^{90}Y- DOTA0-DPhe1-Tyr3-octreotide; ^{90}Y: Yttrium-90.

fect of VDAs either on tumor blood vessels or normal tissues. Lack of complete specificity for tumor-related vasculature or downstream effects induced by cytokines and other released factors can contribute to the toxic signs or effects. A distinctive transient and acute toxicity pattern with minor cumulative side effects such as tumor pain, nausea and vomiting, headaches, vision changes, symptoms associated to serotonin release, neuromotor abnormalities and cerebellar ataxia, acute hemodynamic disturbances, abdominal pain, hypertension, and tachycardia have been reported after VDA administration in clinical trials[91]. The degree and types of the side effects might differ among flavonoids and tubulin-binding agents[91].

So far, combretastatin A-4 phosphate (CA4P), a synthetic phosphorylated derivative of the natural product combretastatin A-4, is a tubulin-binding agent that has been most extensively used in OncoCiDia experiments. In preclinical studies, intravenous CA4P at a dose of 10 mg/kg has shown a complete and rapid vascular shutdown of the tumor with minimal effects at the well-perfused periphery[1,89]. However, some discrepancies have been noted in animal studies and clinical trials concerning the anticancer effect of VDAs[92]. According to the Food and Drug Administration-approved rules for the correct dose calculation[93], such a dose of 10 mg/kg in rodents would be equivalent to 60 mg/m^2 in humans. However, phase I clinical trials of CA4P have demonstrated a minimal objective tumor response by using similar doses of 52 to 68 mg/m^2[94]. The reason for this difference is not yet clear but could be caused by either miscalculations of the dose based on body surface area in mg/m^2 or due to inaccurate dose translation from animal (mg/kg) to humans (mg/m^2) in addition to the less likely interspecies differences. Based on our experiences, we believe that it may hamper the actual potentialities of VDAs for getting desired anticancer effects in human patients if the dose issues are not properly settled. To overcome the problem, an alternative option could be to increase the total injected dose of CA4P but in an approach of multiple small doses for preventing acute side effects[95]. Moreover, since cardiovascular toxicity seems to be with the most toxicity concerns for CA4P[96], pretreatments with high doses of intravenous diltiazem for preventing hypertension accompanied with amlodipine for secondary prophylaxis or nifedipine and atenolol for blocking tachycardia can be also applied[97,98]. Patients taking QT prolonging drugs, or with a history of significant cardiovascular disease, hypokalemia or hypomagnesemia should be handled with great caution[99].

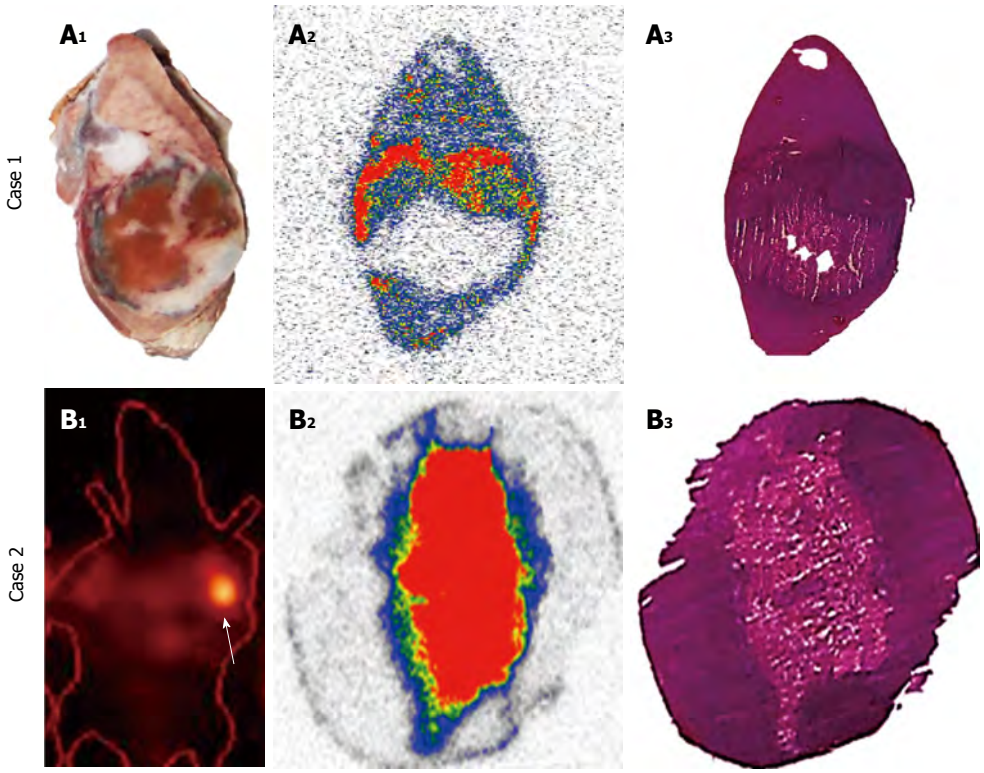

Figure 8 Difference in accumulation patterns of iodine-123/131 labeled hypericin/hypericin in tumor necrosis over time. Case 1: *Ex-vivo* analysis of necrotic tumors from rats with hepatic rhabdomyosarcoma (R1) in the first 24 h after the administration of iodine-123 labeled hypericin/hypericin (^{123}I-Hyp/Hyp) in DMSO/PEG 400/propylene glycol/water (25:25:25:25, v/v/v/v) followed by 1% Evans blue solution. At 24 h after ^{123}I-Hyp/Hyp injection, the tumor necrosis is perfectly outlined by the Evans blue as a blue rim, with viable tumor residues and normal liver with almost no staining (A_1). On the autoradiogram, a perfect match was seen between the high levels of ^{123}I-Hyp/Hyp accumulated in the ring (A_2) and the rim of Evans blue previously observed (A_1). Histology analysis confirms the regions of the liver, necrotic and viable tumors (A_3). Case 2: Single-photon emission computed tomography (SPECT), autoradiograms and histology in severe combined immunodeficiency mice bearing bilateral radiation-induced fibrosarcoma-1 subcutaneously having received combretastatin A-4 phosphate (CA4P) to induce tumor necrosis followed 24 h later by ^{131}I-Hyp/Hyp in DMSO/PEG 400/water (25:60:15, v/v/v). Twelve days after ^{131}I-Hyp/Hyp administration, SPECT detects a persistent intense high radioactivity mainly inside the tumor necrotic core (arrow). Autoradiography (B_2)[1] and histology (B_3) of the tumor after 30 d of tracer injection correspond well with the hotspot imaging on tumor (B_1). [1]The color code bar indicates the coding scheme for the radioactivity. DMSO: Dimethyl sulfoxide; PEG 400: Polyethylene glycol 400.

A study on plasma pharmacokinetics and cerebrospinal fluid penetration of Hyp in rhesus monkeys was conducted. Intravenous administration of 2 mg/kg Hyp was well tolerated. At a dose of 5 mg/kg, a transient severe photosensitivity rash was seen at 12 h that resolved within 12 d[100]. In a phase I study to evaluate the safety and antiretroviral activity of Hyp in thirty HIV-infected patients, weekly repeated IV doses of 0.25 or 0.5 mg/kg were tested. Eleven out of twenty-three patients developed severe cutaneous phototoxicity[101]. In patients with recurrent malignant glioma, a newly developed water soluble formulation of Hyp was IV given (0.1 mg/kg) for tumor visualization. Hyp application proved to be safe with no side effects[102]. Therefore, a low single dose of Hyp at < 0.2 mg/kg for OncoCiDia should be free of noticeable side effects.

I-131 has been used successfully for over 70 years to treat hyperthyroidism and papillary or follicular thyroid cancer and its proper therapeutic use is almost without side effects[103].

However, since accumulation of radioactive iodine was observed in the thyroid, potential damage to the gland could occur due to unnecessary radiation exposure. Therefore, patients undergoing OncoCiDia treatment should take a thyroid-blocking agent on a daily basis before, during and after radiopharmaceutical administration. Either Lugol's solution consisting of elemental iodine and potassium iodide in water or supersaturated potassium iodide solution or oral potassium iodide can be used for this purpose[104].

In a toxicity study with Hyp labeled with non-radioactive iodine (^{127}I), the animals tolerated well IV injections of 0.1 and 10 mg/kg without any signs of clinical toxicity or obvious side effects. The median lethal dose (LD_{50}) of 20.26 mg/kg for ^{127}I-Hyp was above 1000 times of the experimental chemical dose of ^{131}I-Hyp used in OncoCidia, suggesting a wide safety margin with insignificant chemotoxicity[105].

On the other hand, radiation toxic effects could be an issue for ^{131}I-Hyp. Experimental evidence indicated that persistent radioactivity retention mainly occurred in the intestines within few days after injection due to its hepatobiliary excretion[70,75,90]. The acute gastrointestinal syndrome is a main concern following irradiation of the intestinal tract[106]. In a recent study, we tested the suitability of using a newly designed catheter to reduce intestinal

retention of radioactivity after IV administration of ^{131}I-Hyp. Biodistribution and pharmacokinetics of radioiodinated Hyp were also investigated in animals with and without catheterization. In general, the total radioactivity accumulated in the intestines was dramatically reduced by ten times in those animals with catheter placement. Improved tissue biodistribution and kinetic parameters of ^{123}I-Hyp were also seen in cannulated animals. By using this approach, radiation overexposure because of prolonged excretion of ^{131}I-Hyp can be prevented in the future clinical practice[107].

A safety study of IV administered iodogen in DMSO was conducted in mice of both sexes. LD_{50} was determined with iodogen/DMSO doses ranging from 40.0 to 70.0 mg/kg. Toxicity at 30.0 mg/kg was tested for changes in behavior, body weight, and serum biochemistry over 14 d. Due to the toxicity concerns associated with the use of DMSO, a high dose of the solvent was also concurrently tested.

Good safety profile was demonstrated with iodogen in DMSO with LD_{50} values above 50.0 mg/kg and pure DMSO. No animal deaths, pathologies or clinical toxicities were recorded after 30.0 mg/kg iodogen in DMSO, which is 3000 times the dose intended for possible human applications[108].

Overall these data put forward a solid indication for the manageable and tolerable safety of OncoCiDia and potential upcoming clinically applicable formulations in terms of both radiotoxicity and chemotoxicity.

TRANSLATIONAL RESEARCH ON CARDIAC APPLICATIONS OF IODINATED HYPERICIN

Nuclear imaging for diagnosis of myocardial ischemia/infarction

Coronary heart disease, in which MI is a major component, represents the most common cause of death in the Western world. To assess myocardial viability, nuclear imaging uses radiolabelled compounds recognizing specific structures, receptors or antigens to scrutinize the molecular process under physiological conditions in a noninvasive manner. Several myocardial perfusion tracers for single photon emission computed tomography (SPECT) such as thallium-201 (^{201}Tl) and technetium-99m (^{99m}Tc) labeled agents (*e.g.*, sestamibi and tetrofosmin) are currently available in the clinic. They evenly distribute throughout the normal myocardium in proportion to the blood flow, depicting the dead/ischemic tissues as "black spot". However, the development of specific targeting agents with genuine necrosis affinity constitutes an important goal in the management of cardiac pathologies. They may allow early detection, delineation of the infarcted or ischemic area, patient follow-up over-time and evaluation of the response to revascularization therapies[109]. Other cardiovascular diseases related to cardiac cell death could be identified including diverse cardiomyopathy[110], myocardial inflammation, acute myocarditis[111]. Acute or chronic diffuse myocardial damage due to cardiac transplant rejection could also be detected[112].

Various "hot spot" imaging tracers have been exploited for the visualization of MI. Technetium (^{99m}Tc)-pyrophosphate accumulates in necrotic myocardium by targeting the calcium phosphate present in the mitochondria of infarcted or harshly damaged myocardium[113]. ^{99m}Tc-glucarate complex preferentially localizes into basic protein histones within denatured nuclei and subcellular organelles in the dead cardiomyocytes[114]. ^{111}In-labelled monoclonal anti-myosin Fab specifically recognizes the intracellular heavy chain of the exposed cardiac myosin of severely damaged cells[115]. Unfortunately, overestimation of the infarct size due to poor specificity for distinguishing ischemic and necrotic tissues[116,117], and reduced diagnostic accuracy and low target to background ratio on scintigraphic images because of the prompt dissociation of the tracer *in vivo* and short-term accumulation at the damage site[7] have been noticed.

^{123}I-Hyp as a complementary necrosis avid cardiac scintigraphic agent

By micro-single photon emission computed tomography (μSPECT), the potential usefulness of the necrosis avid ^{123}I-Hyp for detection and quantification of acute MI has been reported[118], which is essential for clinical management of ischemic heart disease. In a more recent study[119], ^{123}I-Hyp was compared with the commercial myocardial perfusion agent technetium-99m-labeled-hexakis (2-methoxyisobutylisonitrile) (^{99m}Tc-Sestamibi) in organ distribution and targetability in rabbits with acute MI using dual-isotope simultaneous acquisition-μSPECT/computed tomography and postmortem methods. ^{123}I-Hyp underwent hepatobiliary excretion whereas ^{99m}Tc-Sestamibi distribution was characterized by more rapid hepatorenal elimination. ^{99m}Tc-Sestamibi preferentially accumulated in the normal myocardium, whereas ^{123}I-Hyp confirmed to be a necrosis specific agent that allowed hot spot imaging of irreversibly damaged myocardium or acute MI. Therefore, ^{99m}Tc-Sestamibi and ^{123}I-Hyp can be considered as a pair of complementary tracers for DISA-SPECT/CT in nuclear cardiology[119].

A TRANSLATIONAL APPLICATION ELICITED FROM MECHANISM STUDY ON HYPERICIN

Gallstone basics and pathologies

Cholelithiasis refers to the presence of gallstones in the gallbladder. Although these supersaturated deposits of bile are initially formed within the gallbladder, they may distantly pass into other parts of the biliary tract, reaching the common bile duct, the cystic duct and the pancreatic duct. They can broadly vary in size and appear

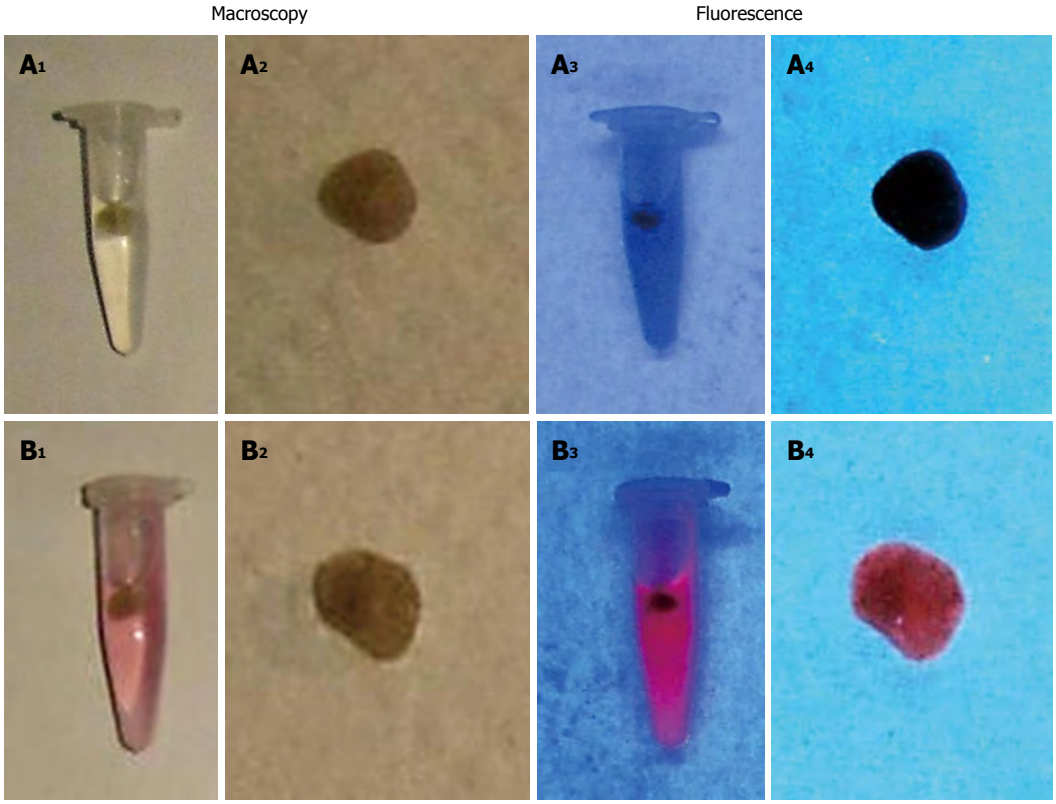

Figure 9 Macroscopic digital imaging of gallbladder stones which were extracted from patients. Stones previously incubated in DMSO/PEG400/water (25:60:15, v/v/v) for 72 h and set as control (A_1, A_2) lack of fluorescent properties (A_3, A_4). Stones treated for 72 h with a solution of Hyp in DMSO/PEG400/water (25:60:15, v/v/v) (B_1, B_2) reveals fluorescence (B_3, B_4) under the UV light of 254 nm. DMSO: Dimethyl sulfoxide; PEG 400: Polyethylene glycol 400; UV: Ultraviolet.

as a single stone or as an assortment of stones with different sizes. Gallstones generally come in three different types including cholesterol stones that represent about 80%, pigment stones composed of bilirubin, the yellow breakdown product of normal heme catabolism found in bile, and mixed stones. Gallstones in the gallbladder may cause acute cholecystitis[120], an inflammatory condition distinguished by bile retention leading to secondary infection by intestinal microorganisms, mainly Escherichia coli, Klebsiella, Enterobacter, and Bacteroides species[121]. Presence of gallstones in the biliary tract can produce obstruction of the bile ducts, leading to severe ascending cholangitis or pancreatitis, which can be life-threatening. Eventually, they can be very painful and may require surgical intervention to remove the gallbladder and/or stones.

Hypericin as an optical imaging agent for fluorescent detection of gallstones

Since Hyp is primarily excreted *via* bile and its interaction with cholesterols has been proved[8,9], the potential use of Hyp as an optical imaging agent for fluorescent detection of gallstones in the clinic was explored. Cholesterol, pigment and mixed gallstones were derived from cholecystectomy patients. *In vitro* studies were conducted by incubating the gallstones with Hyp solutions at increasing concentrations (0-0.01 mg/mL) either in solvent or bile. Under UV light at 254 nm wavelength, red fluorescence was seen on stones previously incubated with Hyp, but this was not observed on only solvent or bile-treated gallstones (Figure 9). The intensity of stone fluorescence depended on Hyp concentration. Although other techniques like ultrasonography or cholescintigraphy scan with ^{99m}Tc-hepatobiliary iminodiacetic acid can usually detect gallstones, the use of Hyp may aid fluorescent detection and removal of gallstones during open and/or endoscopic cholecystectomy and cholangiotomy. *In vivo* studies are needed to prove whether it is a vital and applicable approach.

SAFETY EVALUATION OF MEDICAL DEVICES USING RADIOPHARMACEUTICAL APPROACH

Potential contamination risk from multiple uses of a contrast injection pump

Multiple uses of automatic contrast injection systems for automatic delivery of contrast media during enhanced imaging procedures can reduce costs and save resources. However, cross-contaminations with blood-borne pathogens of infectious diseases may occur[122,123]. To avoid possible nosocomial outbreaks, the injection system including the power syringes, filling and injecting set and

the patient line has to be completely changed for each patient. However, this proves expensive and time consuming due to the wasted surplus contrast materials in the setup from each exam, the consumptions of disposable devices, and the long pauses for changing the entire setup per patient. To reduce material and costs, several institutions worldwide have been applying multiple usages of the syringes with automatic injectors for serial patients. Generally, these commercially available injection systems contain a special one-way-valve tube device. However, nosocomial outbreaks between patients are still a problem because of contamination of the injection system with blood-borne pathogen[124].

A radioactive method for assessing microbial safety of an infusion set

The purpose of this experiment was to develop a radioactive method for quantitative safety evaluation of a new replaceable patient-delivery system[125]. This system (Transflux™ Diepenbeek, Belgium) contains a safety zone composed by a tube and two one-way valves. It permits to flush the whole injector system and the vein but prevents blood reflux during contrast-enhanced imaging. This system is replaced for each new patient, whereas the power syringes need to be changed only once a day after multiple uses for a series of patients. It has been applied for years in many radiology units without any contaminative infections reported, which though has to be experimentally justified.

By mimicking pathogens with a diffusible radiotracer, we evaluated the feasibility of using this system repeatedly without septic risks. The experiment was performed by intravenous injection of ^{99m}Tc-dimercaptopropionyl-human serum albumin in rabbits previously connected *via* an endovenous catheter to an automatic contrast injection system. Protocols with normal saline and contrast agent plus saline loaded in the injection system were compared. By sampling and analyzing aliquots from the filling and injecting set, patient line and blood, it was checked if the radiotracer from the patient line in contact with animal blood was able to cross the safety zone and reach the power syringes.

Overall, with both protocols, radioactivity was found in blood and in patient line but in none of the samples from the filling-injecting set. This radioactive method appears accurate and reliable. The patient-delivery system proves safe and convenient, which is in line with the clinical experiences collected to date. By replacing the patient delivery system, cross-contamination risks can be avoided without changing the main part of injection system. This method can be applied for evaluation of similar devices before human use.

CONCLUSION

Translational medicine aims at identifying solutions to specific health problems. Different but important difficulties faced in cancer treatment, identification of cardiac infarction, detection of cholelithiasis and safety evaluation of medical devices might be considerably tackled by well-designed laboratory experiments.

OncoCiDia presents an unconventional but general approach based on the necrosis avidity for treating multifocal and multitype malignant tumors. It uses a combined sequence of a vascular disrupting agent for triggering massive tumor necrosis followed by the necrosis avid ^{131}I-Hyp to destroy remaining tumor cells. Some technical optimizations have been performed and herein demonstrated to assist in introducing OncoCiDia to the possible clinical practice. The feasible Hyp radioiodination with good radiochemical yields and a proper formulation for *in vivo* applications have been investigated and discussed. The favorable biodistribution, dosimetry and pharmacokinetic patterns as well as good *in vivo* tolerance and low toxicity of radioiodinated Hyp have been exhibited in animal experiments. In general, the genuine benefits of ^{131}I-Hyp distinguished by high and unprecedented long-term accumulation in tumor necrosis in the vicinity of cancer cells and its convenient clearance mechanism through bile without renal retention could noticeably impact on cancer theragnostic management or open doors for handling a wide diversity of cancers in future clinical practice.

Targeting necrosis may offer new opportunities for the management of cardiac pathologies. The clinical introduction of radioactive necrosis-specific agents like ^{123}I-Hyp might play a complementary role in detection and quantification of acute myocardial infarction. The combination of the genuine ^{123}I-Hyp necrosis avidity with the preferential uptake of the currently used commercial myocardial perfusion agent by normal myocardium might offer additional information in the clinical management of this life-threatening pathology.

On the other hand, the use of the fluorophore hypericin as an optical imaging agent with low *in vivo* toxicity could be an excellent diagnostic tool for the detection and removal of gallstones in patients suffering from such common clinical conditions.

Finally, the risk of accidental cross-contamination in medical devices can be minimized through safety evaluation studies based on the inherent sensitivity of radioactive methods in preclinical animal experiments.

REFERENCES

1 **Li J**, Sun Z, Zhang J, Shao H, Cona MM, Wang H, Marysael T, Chen F, Prinsen K, Zhou L, Huang D, Nuyts J, Yu J, Meng B, Bormans G, Fang Z, de Witte P, Li Y, Verbruggen A, Wang X, Mortelmans L, Xu K, Marchal G, Ni Y. A dual-targeting anticancer approach: soil and seed principle. *Radiology* 2011; **260**: 799-807 [PMID: 21712473 DOI: 10.1148/radiol.11102120]

2 **Aschylus.** OncoCidia. Available from: URL: http: //www.aeschylus-philanthropy.eu/index.php/b/project/oncocidia

3 **Roger VL.** Epidemiology of myocardial infarction. *Med Clin North Am* 2007; 91: 537–552 [DOI: 10.1016/j.mcna.2007.03.007]

4 **Bauer A**, Mehilli J, Barthel P, Müller A, Kastrati A, Ulm K, Schömig A, Malik M, Schmidt G. Impact of myocardial salvage assessed by (99m)Tc-sestamibi scintigraphy on car-

diac autonomic function in patients undergoing mechanical reperfusion therapy for acute myocardial infarction. *JACC Cardiovasc Imaging* 2009; **2**: 449-457 [PMID: 19580728 DOI: 10.1016/j.jcmg.2008.12.018]

5 **Lombardo A**, Rizzello V, Galiuto L, Natale L, Giordano A, Rebuzzi A, Loperfido F, Crea F, Maseri A. Assessment of resting perfusion defects in patients with acute myocardial infarction: comparison of myocardial contrast echocardiography, combined first-pass/delayed contrast-enhanced magnetic resonance imaging and 99mTC-sestamibi SPECT. *Int J Cardiovasc Imaging* 2006; **22**: 417-428 [PMID: 16496094 DOI: 10.1007/s10554-005-9045-8]

6 **Ni Y,** Bormans G, Marchal G, Verbruggen A. Tissue infarction and necrosis specific compounds (of hypericin derivatives). Available from: URL: http://www.google.com/patents/EP1651201B1

7 **Ni Y**, Huyghe D, Verbeke K, de Witte PA, Nuyts J, Mortelmans L, Chen F, Marchal G, Verbruggen AM, Bormans GM. First preclinical evaluation of mono-[123I]iodohypericin as a necrosis-avid tracer agent. *Eur J Nucl Med Mol Imaging* 2006; **33**: 595-601 [PMID: 16450141 DOI: 10.1007/s00259-005-0013-2]

8 **Ho YF**, Wu MH, Cheng BH, Chen YW, Shih MC. Lipid-mediated preferential localization of hypericin in lipid membranes. *Biochim Biophys Acta* 2009; **1788**: 1287-1295 [PMID: 19366588 DOI: 10.1016/j.bbamem.2009.01.017]

9 **Eriksson ESE,** Eriksson LA. The influence of cholesterol on the properties and permeability of hypericin derivatives in lipid membranes. J. *Chem Theory Comput* 2011; **7**: 560–574 [DOI: 10.1021/ct100528u]

10 **Cancer Research UK.** Cancer Worldwide - the global picture. Future trends. Available from: URL: http: //www.cancerresearchuk.org/cancer-info/cancerstats/world/cancer-worldwide-the-global-picture

11 **Luster M**, Clarke SE, Dietlein M, Lassmann M, Lind P, Oyen WJ, Tennvall J, Bombardieri E. Guidelines for radioiodine therapy of differentiated thyroid cancer. *Eur J Nucl Med Mol Imaging* 2008; **35**: 1941-1959 [PMID: 18670773 DOI: 10.1007/s00259-008-0883-1]

12 **Gedik GK**, Hoefnagel CA, Bais E, Olmos RA. 131I-MIBG therapy in metastatic phaeochromocytoma and paraganglioma. *Eur J Nucl Med Mol Imaging* 2008; **35**: 725-733 [PMID: 18071700 DOI: 10.1007/s00259-007-0652-6]

13 **Polishchuk AL**, Dubois SG, Haas-Kogan D, Hawkins R, Matthay KK. Response, survival, and toxicity after iodine-131-metaiodobenzylguanidine therapy for neuroblastoma in preadolescents, adolescents, and adults. *Cancer* 2011; **117**: 4286-4293 [PMID: 21387264 DOI: 10.1002/cncr.25987]

14 **McEwan AJ**, Amyotte GA, McGowan DG, MacGillivray JA, Porter AT. A retrospective analysis of the cost effectiveness of treatment with Metastron (89Sr-chloride) in patients with prostate cancer metastatic to bone. *Nucl Med Commun* 1994; **15**: 499-504 [PMID: 7970425]

15 **Rhee TK**, Lewandowski RJ, Liu DM, Mulcahy MF, Takahashi G, Hansen PD, Benson AB, Kennedy AS, Omary RA, Salem R. 90Y Radioembolization for metastatic neuroendocrine liver tumors: preliminary results from a multi-institutional experience. *Ann Surg* 2008; **247**: 1029-1035 [PMID: 18520231 DOI: 10.1097/SLA.0b013e3181728a45]

16 **Smith K**, Byer G, Morris CG, Kirwan JM, Lightsey J, Mendenhall NP, Hoppe BS, Lynch J, Olivier K. Outcomes of patients with non-Hodgkin's lymphoma treated with Bexxar with or without external-beam radiotherapy. *Int J Radiat Oncol Biol Phys* 2012; **82**: 1122-1127 [PMID: 21570217 DOI: 10.1016/j.ijrobp.2010.09.044]

17 **Micallef IN**. Ongoing trials with yttrium 90-labeled ibritumomab tiuxetan in patients with non-Hodgkin's lymphoma. *Clin Lymphoma* 2004; **5** Suppl 1: S27-S32 [PMID: 15498147]

18 **Virgolini I**, Traub T, Novotny C, Leimer M, Füger B, Li SR, Patri P, Pangerl T, Angelberger P, Raderer M, Burggasser G, Andreae F, Kurtaran A, Dudczak R. Experience with indium-111 and yttrium-90-labeled somatostatin analogs. *Curr Pharm Des* 2002; **8**: 1781-1807 [PMID: 12171531 DOI: 10.2174/1381612023393756]

19 **Kwekkeboom DJ**, Kam BL, van Essen M, Teunissen JJ, van Eijck CH, Valkema R, de Jong M, de Herder WW, Krenning EP. Somatostatin-receptor-based imaging and therapy of gastroenteropancreatic neuroendocrine tumors. *Endocr Relat Cancer* 2010; **17**: R53-R73 [PMID: 19995807 DOI: 10.1677/ERC-09-0078]

20 **Paganelli G**, Chinol M. Radioimmunotherapy: is avidin-biotin pretargeting the preferred choice among pretargeting methods? *Eur J Nucl Med Mol Imaging* 2003; **30**: 773-776 [PMID: 12557049 DOI: 10.1007/s00259-002-1090-0]

21 **Sharkey RM**. Radioimmunotherapy against the tumor vasculature: A new target? *J Nucl Med* 2006; **47**: 1070-1074 [PMID: 16818938]

22 **Govindan SV**, Goldenberg DM, Hansen HJ, Griffiths GL. Advances in the use of monoclonal antibodies in cancer radiotherapy. *Pharm Sci Technolo Today* 2000; **3**: 90-98 [PMID: 10707044 DOI: 10.1016/S1461-5347(00)00241-8]

23 **Ginj M**, Zhang H, Waser B, Cescato R, Wild D, Wang X, Erchegyi J, Rivier J, Mäcke HR, Reubi JC. Radiolabeled somatostatin receptor antagonists are preferable to agonists for in vivo peptide receptor targeting of tumors. *Proc Natl Acad Sci USA* 2006; **103**: 16436-16441 [PMID: 17056720 DOI: 10.1073/pnas.0607761103]

24 **Merlo LM**, Pepper JW, Reid BJ, Maley CC. Cancer as an evolutionary and ecological process. *Nat Rev Cancer* 2006; **6**: 924-935 [PMID: 17109012 DOI: 10.1038/nrc2013]

25 **Aggarwal BB**, Danda D, Gupta S, Gehlot P. Models for prevention and treatment of cancer: problems vs promises. *Biochem Pharmacol* 2009; **78**: 1083-1094 [PMID: 19481061 DOI: 10.1016/j.bcp.2009.05.027]

26 **Hornick JL**, Sharifi J, Khawli LA, Hu P, Biela BH, Mizokami MM, Yun A, Taylor CR, Epstein AL. A new chemically modified chimeric TNT-3 monoclonal antibody directed against DNA for the radioimmunotherapy of solid tumors. *Cancer Biother Radiopharm* 1998; **13**: 255-268 [PMID: 10850361]

27 **Epstein AL**, Chen FM, Taylor CR. A novel method for the detection of necrotic lesions in human cancers. *Cancer Res* 1988; **48**: 5842-5848 [PMID: 3048650]

28 **Charbit A**, Malaise EP, Tubiana M. Relation between the pathological nature and the growth rate of human tumors. *Eur J Cancer* 1971; **7**: 307-315 [PMID: 4328281 DOI: 10.1016/0014-2964(71)90073-9]

29 **Malaise EP**, Chavaudra N, Tubiana M. The relationship between growth rate, labelling index and histological type of human solid tumours. *Eur J Cancer* 1973; **9**: 305-312 [PMID: 4360278 DOI: 10.1016/0014-2964]

30 **Miller GK**, Naeve GS, Gaffar SA, Epstein AL. Immunologic and biochemical analysis of TNT-1 and TNT-2 monoclonal antibody binding to histones. *Hybridoma* 1993; **12**: 689-698 [PMID: 8288270 DOI: 10.1089/hyb.1993.12.689]

31 **Chen FM**, Taylor CR, Epstein AL. Tumor necrosis treatment of ME-180 human cervical carcinoma model with 131I-labeled TNT-1 monoclonal antibody. *Cancer Res* 1989; **49**: 4578-4585 [PMID: 2743341]

32 **Kanduc D**, Mittelman A, Serpico R, Sinigaglia E, Sinha AA, Natale C, Santacroce R, Di Corcia MG, Lucchese A, Dini L, Pani P, Santacroce S, Simone S, Bucci R, Farber E. Cell death: apoptosis versus necrosis (review). *Int J Oncol* 2002; **21**: 165-170 [PMID: 12063564]

33 **Kroemer G**, Galluzzi L, Vandenabeele P, Abrams J, Alnemri ES, Baehrecke EH, Blagosklonny MV, El-Deiry WS, Golstein P, Green DR, Hengartner M, Knight RA, Kumar S, Lipton SA, Malorni W, Nuñez G, Peter ME, Tschopp J, Yuan J, Piacentini M, Zhivotovsky B, Melino G. Classification of cell death: recommendations of the Nomenclature Committee on Cell Death 2009. *Cell Death Differ* 2009; **16**: 3-11 [PMID: 18846107 DOI: 10.1038/cdd.2008.150]

34 **Walker NI**, Harmon BV, Gobé GC, Kerr JF. Patterns of cell death. *Methods Achiev Exp Pathol* 1988; **13**: 18-54 [PMID: 3045494]

35 **Hitomi J**, Christofferson DE, Ng A, Yao J, Degterev A, Xavier RJ, Yuan J. Identification of a molecular signaling network that regulates a cellular necrotic cell death pathway. *Cell* 2008; **135**: 1311-1323 [PMID: 19109899 DOI: 10.1016/j.cell.2008.10.044]

36 **Wu W**, Liu P, Li J. Necroptosis: an emerging form of programmed cell death. *Crit Rev Oncol Hematol* 2012; **82**: 249-258 [PMID: 21962882 DOI: 10.1016/j.critrevonc.2011.08.004]

37 **Degterev A,** Huang Z, Boyce M, Li Y, Jagtap P, Mizushima N, Cuny GD, Mitchison TJ, Moskowitz MA, Yuan J. Chemical inhibitor of nonapoptotic cell death with therapeutic potential for ischemic brain injury. *Nat Chem Biol* 2005; **1**: 112-119 [DOI: 10.1038/nchembio711]

38 **Yu L**, Alva A, Su H, Dutt P, Freundt E, Welsh S, Baehrecke EH, Lenardo MJ. Regulation of an ATG7-beclin 1 program of autophagic cell death by caspase-8. *Science* 2004; **304**: 1500-1502 [PMID: 15131264 DOI: 10.1126/science.1096645]

39 **Cho YS**, Challa S, Moquin D, Genga R, Ray TD, Guildford M, Chan FK. Phosphorylation-driven assembly of the RIP1-RIP3 complex regulates programmed necrosis and virus-induced inflammation. *Cell* 2009; **137**: 1112-1123 [PMID: 19524513 DOI: 10.1016/j.cell.2009.05.037]

40 **Nanji AA**, Hiller-Sturmhöfel S. Apoptosis and necrosis: two types of cell death in alcoholic liver disease. *Alcohol Health Res World* 1997; **21**: 325-330 [PMID: 15706744]

41 **Ziegler U**, Groscurth P. Morphological features of cell death. *News Physiol Sci* 2004; **19**: 124-128 [PMID: 15143207 DOI: 10.1152/nips.01519.2004]

42 **Human pathology.** Available from: URL: http: //www.humpath.com/spip.php?article4548

43 **Street HH**, Goris ML, Fisher GA, Wessels BW, Cho C, Hernandez C, Zhu HJ, Zhang Y, Nangiana JS, Shan JS, Roberts K, Knox SJ. Phase I study of 131I-chimeric(ch) TNT-1/B monoclonal antibody for the treatment of advanced colon cancer. *Cancer Biother Radiopharm* 2006; **21**: 243-256 [PMID: 16918301 DOI: 10.1089/cbr.2006.21.243]

44 **Hdeib A**, Sloan AE. Convection-enhanced delivery of 131I-chTNT-1/B mAB for treatment of high-grade adult gliomas. *Expert Opin Biol Ther* 2011; **11**: 799-806 [PMID: 21521146 DOI: 10.1517/14712598.2011.579097]

45 **Chen S**, Yu L, Jiang C, Zhao Y, Sun D, Li S, Liao G, Chen Y, Fu Q, Tao Q, Ye D, Hu P, Khawli LA, Taylor CR, Epstein AL, Ju DW. Pivotal study of iodine-131-labeled chimeric tumor necrosis treatment radioimmunotherapy in patients with advanced lung cancer. *J Clin Oncol* 2005; **23**: 1538-1547 [PMID: 15735129 DOI: 10.1200/JCO.2005.06.108]

46 **Khawli LA**, Alauddin MM, Hu P, Epstein AL. Tumor targeting properties of indium-111 labeled genetically engineered Fab′ and F(ab′)2 constructs of chimeric tumor necrosis treatment (chTNT)-3 antibody. *Cancer Biother Radiopharm* 2003; **18**: 931-940 [PMID: 14969605 DOI: 10.1089/108497803322702897]

47 **Anderson PM,** Wiseman GA, Lewis BD, Charboneau W, Dunn WL, Carpenter SP, Chew T. A phase I safety and imaging study using radiofrequency ablation (RFA) followed by 131I-chTNT-1/B radioimmunotherapy adjuvant treatment of hepatic metastases. *Cancer Ther* 2003; **1**: 283-291

48 **Tozer GM**, Kanthou C, Baguley BC. Disrupting tumour blood vessels. *Nat Rev Cancer* 2005; **5**: 423-435 [PMID: 15928673 DOI: 10.1038/nrc1628]

49 **Chaplin DJ**, Hill SA. The development of combretastatin A4 phosphate as a vascular targeting agent. *Int J Radiat Oncol Biol Phys* 2002; **54**: 1491-1496 [PMID: 12459376 DOI: 10.1016/S0360-3016(02)03924-X]

50 **Chaplin DJ**, Dougherty GJ. Tumour vasculature as a target for cancer therapy. *Br J Cancer* 1999; **80** Suppl 1: 57-64 [PMID: 10466764]

51 **Siemann DW**, Bibby MC, Dark GG, Dicker AP, Eskens FA, Horsman MR, Marmé D, Lorusso PM. Differentiation and definition of vascular-targeted therapies. *Clin Cancer Res* 2005; **11**: 416-420 [PMID: 15701823]

52 **Karioti A**, Bilia AR. Hypericins as potential leads for new therapeutics. *Int J Mol Sci* 2010; **11**: 562-594 [PMID: 20386655 DOI: 10.3390/ijms11020562]

53 **Wolfender JL,** Queiroz EF, Hostettmann K. Photochemistry. In: Birkhäuser Verlag. St. John's Wort and its Active Principles in Depression and Anxiety. Basel, 2005: 5-19

54 **Dewick PM.** Aromatic Polyketides. Structural Modifications: Anthraquinones. In: Jonh Wiley & Sons Ltd. Medicinal natural products: a biosynthetic approach, 2nd ed. West Sussex, 2002: 63-71

55 **Leonhartsberger JG,** Falk H. The protonation and deprotonation equilibria of hypericin revisited. *Monatsh Chem* 2002; **133**: 167–172 [DOI: 10.1007/s706-002-8246-x]

56 **Etzlstorfer C,** Falk H, Müller N, Schmitzberger W, Wagner UG. Tautomerism and stereochemistry of hypericin: Force field, NMR, and X-ray crystallographic investigations. *Monatsh Chemie* 1993; **124**: 751-761 [DOI: 10.1007/BF00817311]

57 **Gutman I,** Marković Z, Solujić S, Sukdolak S. On the tautomers of hypericin. chemistry and materials science. *Monatshefte fur Chemie* 1998; **129**: 481-486 [DOI: 10.1007/PL00000105]

58 **Kapinus EI**, Falk H, Tran HTN. Spectroscopic investigation of the molecular structure of hypericin and its salts. *Monatshefte fuÈr Chemie* 1999; **130**: 623-635 [DOI: 10.1007/PL00010243]

59 **Bánó G**, Staničová J, Jancura D, Marek J, Bánó M, Uličný J, Strejčková A, Miškovský P. On the diffusion of hypericin in dimethylsulfoxide/water mixtures-the effect of aggregation. *J Phys Chem B* 2011; **115**: 2417-2423 [PMID: 21332112 DOI: 10.1021/jp109661c]

60 **Buriankova L**, Buzova D, Chorvat D, Sureau F, Brault D, Miskovský P, Jancura D. Kinetics of hypericin association with low-density lipoproteins. *Photochem Photobiol* 2011; **87**: 56-63 [PMID: 21114669 DOI: 10.1111/j.1751-1097.2010.00847.x]

61 **Sosa S**, Pace R, Bornancin A, Morazzoni P, Riva A, Tubaro A, Della Loggia R. Topical anti-inflammatory activity of extracts and compounds from Hypericum perforatum L. *J Pharm Pharmacol* 2007; **59**: 703-709 [PMID: 17524236 DOI: 10.1211/jpp.59.5.0011]

62 **Meruelo D**, Lavie G, Lavie D. Therapeutic agents with dramatic antiretroviral activity and little toxicity at effective doses: aromatic polycyclic diones hypericin and pseudohypericin. *Proc Natl Acad Sci USA* 1988; **85**: 5230-5234 [PMID: 2839837]

63 **Avato P**, Raffo F, Guglielmi G, Vitali C, Rosato A. Extracts from St John's Wort and their antimicrobial activity. *Phytother Res* 2004; **18**: 230-232 [PMID: 15103670 DOI: 10.1002/ptr.1430]

64 **Blank M**, Mandel M, Hazan S, Keisari Y, Lavie G. Anticancer activities of hypericin in the dark. *Photochem Photobiol* 2001; **74**: 120-125 [PMID: 11547544 DOI: 10.1562/0031-8655(2001)0740120AC]

65 **Linde K**, Ramirez G, Mulrow CD, Pauls A, Weidenhammer W, Melchart D. St John's wort for depression--an overview and meta-analysis of randomised clinical trials. *BMJ* 1996; **313**: 253-258 [PMID: 8704532 DOI: 10.1136/bmj.313.7052.253]

66 **Ni Y**, Bormans G, Chen F, Verbruggen A, Marchal G. Necrosis avid contrast agents: functional similarity versus structur-

al diversity. *Invest Radiol* 2005; **40**: 526-535 [PMID: 16024991]
67 **Miskovsky P**, Hritz J, Sanchez-Cortes S, Fabriciova G, Ulicny J, Chinsky L. Interaction of hypericin with serum albumins: surface-enhanced Raman spectroscopy, resonance Raman spectroscopy and molecular modeling study. *Photochem Photobiol* 2001; **74**: 172-183 [PMID: 11547551 DOI: 10.1562/0031-8655(2001)0740172IO]
68 **Song S**, Xiong C, Zhou M, Lu W, Huang Q, Ku G, Zhao J, Flores LG, Ni Y, Li C. Small-animal PET of tumor damage induced by photothermal ablation with 64Cu-bis-DOTA-hypericin. *J Nucl Med* 2011; **52**: 792-799 [PMID: 21498539 DOI: 10.2967/jnumed.110.086116]
69 **Loke KS**, Padhy AK, Ng DC, Goh AS, Divgi C. Dosimetric considerations in radioimmunotherapy and systemic radionuclide therapies: a review. *World J Nucl Med* 2011; **10**: 122-138 [PMID: 22144871 DOI: 10.4103/1450-1147.89780]
70 **Bormans G,** Huyghe D, Christiaen A, Verbeke K, de Groot T, Vanbilloen H, de Witte P, Verbruggen A. Preparation, analysis and biodistribution in mice of iodine-123 labeled derivatives of hypericin. *Journal of Labeled Compounds and Radiopharmaceuticals* 2004; **47**: 191–198 [DOI: 10.1002/jlcr.812]
71 **Sun ZP,** inventor. Iodogen method for preparation of radioiodinated Hypericin. Available from: URL: http://www.google.com/patents/CN101475461B?cl=zh
72 **Sihver W**, Bier D, Holschbach MH, Schulze A, Wutz W, Olsson RA, Coenen HH. Binding of tritiated and radioiodinated ZM241,385 to brain A2A adenosine receptors. *Nucl Med Biol* 2004; **31**: 173-177 [PMID: 15013482 DOI: 10.1016/j.nucmedbio.2003.10.007]
73 **Emami B**, Lyman J, Brown A, Coia L, Goitein M, Munzenrider JE, Shank B, Solin LJ, Wesson M. Tolerance of normal tissue to therapeutic irradiation. *Int J Radiat Oncol Biol Phys* 1991; **21**: 109-122 [PMID: 2032882 DOI: 10.1016/0360-3016(91)90171-Y]
74 **Li J**, Cona MM, Chen F, Feng Y, Zhou L, Yu J, Nuyts J, de Witte P, Zhang J, Himmelreich U, Verbruggen A, Ni Y. Exploring theranostic potentials of radioiodinated hypericin in rodent necrosis models. *Theranostics* 2012; **2**: 1010-1019 [PMID: 23139728 DOI: 10.7150/thno.4924]
75 **Cona MM,** Li J, Bauwens M, Feng Y, Sun Z, Zhang J, Chen F, Alpizar Y, Talavera K, de Witte P, Verbruggen A, Oyen R, Ni Y. Radioiodinated Hypericin: Its Biodistribution, Necrosis Avidity and Therapeutic Efficacy are Influenced by Formulation. *Pharm Res* 2013 Aug 9; Epub ahead of print [PMID: 23934256 DOI: 10.1007/s11095-013-1159-4]
76 **Laurent A**, Mottu F, Chapot R, Zhang JQ, Jordan O, Rüfenacht DA, Doelker E, Merland JJ. Cardiovascular effects of selected water-miscible solvents for pharmaceutical injections and embolization materials: a comparative hemodynamic study using a sheep model. *PDA J Pharm Sci Technol* 2007; **61**: 64-74 [PMID: 17479714]
77 **Reed KW**, Yalkowsky SH. Lysis of human red blood cells in the presence of various cosolvents. III. The relationship between hemolytic potential and structure. *J Parenter Sci Technol* 1987; **41**: 37-39 [PMID: 3559834]
78 **Conte G,** Di Blasi R, Giglio E, Parretta A, Pavel NV. Nuclear magnetic resonance and x-ray studies on micellar aggregates of sodium deoxycholate. *J Phys Chem* 1984; **88**: 5720–5724 [DOI: 10.1021/j150667a052]
79 **Miranda Cona M,** Feng YB, Jian Zhang, Yue Li, Verbruggen A, Oyen R, Ni Y. Sodium cholate, a solubilizing agent for the necrosis avid radioiodinated hypericin in rabbits with acute myocardial infarction. *Drug Delivery* 2014; (in press) [DOI: 10.3109/10717544.2013.873838]
80 **Miranda Cona M,** Koole M, Feng YB, Liu YW, Verbruggen A, Oyen R and Ni Y. Biodistribution and radiation dosimetry of radioiodinated hypericin as a cancer therapeutic. *International Journal of Oncology* 2014; 44 (in press) [DOI: 10.3892/ijo.2013.2217]
81 **Seo Y**, Gustafson WC, Dannoon SF, Nekritz EA, Lee CL, Murphy ST, VanBrocklin HF, Hernandez-Pampaloni M, Haas-Kogan DA, Weiss WA, Matthay KK. Tumor dosimetry using [124I]m-iodobenzylguanidine microPET/CT for [131I]m-iodobenzylguanidine treatment of neuroblastoma in a murine xenograft model. *Mol Imaging Biol* 2012; **14**: 735-742 [PMID: 22382618 DOI: 10.1007/s11307-012-0552-4]
82 **Koppe MJ**, Bleichrodt RP, Soede AC, Verhofstad AA, Goldenberg DM, Oyen WJ, Boerman OC. Biodistribution and therapeutic efficacy of (125/131)I-, (186)Re-, (88/90)Y-, or (177)Lu-labeled monoclonal antibody MN-14 to carcinoembryonic antigen in mice with small peritoneal metastases of colorectal origin. *J Nucl Med* 2004; **45**: 1224-1232 [PMID: 15235070]
83 **Kaminski MS**, Estes J, Zasadny KR, Francis IR, Ross CW, Tuck M, Regan D, Fisher S, Gutierrez J, Kroll S, Stagg R, Tidmarsh G, Wahl RL. Radioimmunotherapy with iodine (131)I tositumomab for relapsed or refractory B-cell non-Hodgkin lymphoma: updated results and long-term follow-up of the University of Michigan experience. *Blood* 2000; **96**: 1259-1266 [PMID: 10942366]
84 **Persson M**, Rasmussen P, Madsen J, Ploug M, Kjaer A. New peptide receptor radionuclide therapy of invasive cancer cells: in vivo studies using 177Lu-DOTA-AE105 targeting uPAR in human colorectal cancer xenografts. *Nucl Med Biol* 2012; **39**: 962-969 [PMID: 22739362 DOI: 10.1016/j.nucmedbio.2012.05.007]
85 **Persson M**, Gedda L, Lundqvist H, Tolmachev V, Nordgren H, Malmström PU, Carlsson J. [177Lu]pertuzumab: experimental therapy of HER-2-expressing xenografts. *Cancer Res* 2007; **67**: 326-331 [PMID: 17210714 DOI: 10.1158/0008-5472.CAN-06-2363]
86 **Argyrou M,** Valassi A, Andreou M, Lyra M. Dosimetry and therapeutic ratios for rhenium-186 HEDP. *ISRN Molecular Imaging* 2013; **2013**: 1-6 [DOI: 10.1155/2013/124603]
87 **Rizvi SN**, Visser OJ, Vosjan MJ, van Lingen A, Hoekstra OS, Zijlstra JM, Huijgens PC, van Dongen GA, Lubberink M. Biodistribution, radiation dosimetry and scouting of 90Y-ibritumomab tiuxetan therapy in patients with relapsed B-cell non-Hodgkin's lymphoma using 89Zr-ibritumomab tiuxetan and PET. *Eur J Nucl Med Mol Imaging* 2012; **39**: 512-520 [PMID: 22218876 DOI: 10.1007/s00259-011-2008-5]
88 **Cremonesi M,** Ferrari M, Bodei L, Tosi G, Paganelli G. Dosimetry in Peptide radionuclide receptor therapy: a review. *J Nucl Med* 2006; **47**: 1467-1475 [PMID: 16954555]
89 **Li J**, Cona MM, Chen F, Feng Y, Zhou L, Zhang G, Nuyts J, de Witte P, Zhang J, Yu J, Oyen R, Verbruggen A, Ni Y. Sequential systemic administrations of combretastatin A4 Phosphate and radioiodinated hypericin exert synergistic targeted theranostic effects with prolonged survival on SCID mice carrying bifocal tumor xenografts. *Theranostics* 2013; **3**: 127-137 [PMID: 23423247 DOI: 10.7150/thno.5790]
90 **Cona MM,** Li J, Feng Y, Chen F, Verbruggen A, de Witte P, Oyen R, Ni Y. Targetability and Biodistribution of Radioiodinated Hypericin: Comparison between microdosing and carrier-added preparations. *Anticancer Agents Med Chem* 2013 Aug 28; Epub ahead of print [PMID: 24102315]
91 **Hasani A**, Leighl N. Classification and toxicities of vascular disrupting agents. *Clin Lung Cancer* 2011; **12**: 18-25 [PMID: 21273175 DOI: 10.3816/CLC.2011.n.002]
92 **Felici A**, Verweij J, Sparreboom A. Dosing strategies for anticancer drugs: the good, the bad and body-surface area. *Eur J Cancer* 2002; **38**: 1677-1684 [PMID: 12175683 DOI: 10.1016/S0959-8049(02)00151-X]
93 **Reagan-Shaw S**, Nihal M, Ahmad N. Dose translation from animal to human studies revisited. *FASEB J* 2008; **22**: 659-661 [PMID: 17942826 DOI: 10.1096/fj.07-9574LSF]
94 **Ng QS**, Mandeville H, Goh V, Alonzi R, Milner J, Carnell D, Meer K, Padhani AR, Saunders MI, Hoskin PJ. Phase Ib trial of radiotherapy in combination with combretastatin-A4-phosphate in patients with non-small-cell lung cancer, prostate adenocarcinoma, and squamous cell carcinoma of the

head and neck. *Ann Oncol* 2012; **23**: 231-237 [PMID: 21765046 DOI: 10.1093/annonc/mdr332]
95 **Burke JM**, Miller JE. Evaluation of multiple low doses of copper oxide wire particles compared with levamisole for control of Haemonchus contortus in lambs. *Vet Parasitol* 2006; **139**: 145-149 [PMID: 16574324]
96 **Subbiah IM**, Lenihan DJ, Tsimberidou AM. Cardiovascular toxicity profiles of vascular-disrupting agents. *Oncologist* 2011; **16**: 1120-1130 [PMID: 21742963 DOI: 10.1634/theoncologist.2010-0432]
97 **Zweifel M,** Zweifel M, Jayson GC, Reed NS, Osborne R, Hassan B, Ledermann J, Shreeves G, Poupard L, Lu SP, Balkissoon J, Chaplin DJ, Rustin GJ. Phase II trial of combretastatin A4 phosphate, carboplatin, and paclitaxel in patients with platinum-resistant ovarian cancer. *Ann Oncol* 2011; **22**: 2036-2041 [PMID:21273348 DOI: 10.1093/annonc/mdq708]
98 **Gould S**, Westwood FR, Curwen JO, Ashton SE, Roberts DW, Lovick SC, Ryan AJ. Effect of pretreatment with atenolol and nifedipine on ZD6126-induced cardiac toxicity in rats. *J Natl Cancer Inst* 2007; **99**: 1724-1728 [PMID: 18000220 DOI: 10.1093/jnci/djm202]
99 **Rustin GJ**, Galbraith SM, Anderson H, Stratford M, Folkes LK, Sena L, Gumbrell L, Price PM. Phase I clinical trial of weekly combretastatin A4 phosphate: clinical and pharmacokinetic results. *J Clin Oncol* 2003; **21**: 2815-2822 [PMID: 12807934 DOI: 10.1200/JCO.2003.05.185]
100 **Fox E**, Murphy RF, McCully CL, Adamson PC. Plasma pharmacokinetics and cerebrospinal fluid penetration of hypericin in nonhuman primates. *Cancer Chemother Pharmacol* 2001; **47**: 41-44 [PMID: 11221960 DOI: 10.1007/s002800000188]
101 **Gulick RM**, McAuliffe V, Holden-Wiltse J, Crumpacker C, Liebes L, Stein DS, Meehan P, Hussey S, Forcht J, Valentine FT. Phase I studies of hypericin, the active compound in St. John's Wort, as an antiretroviral agent in HIV-infected adults. AIDS Clinical Trials Group Protocols 150 and 258. *Ann Intern Med* 1999; **130**: 510-514 [PMID: 10075619 DOI: 10.7326/0003-4819-130-6-199903160-00015]
102 **Ritz R**, Daniels R, Noell S, Feigl GC, Schmidt V, Bornemann A, Ramina K, Mayer D, Dietz K, Strauss WS, Tatagiba M. Hypericin for visualization of high grade gliomas: first clinical experience. *Eur J Surg Oncol* 2012; **38**: 352-360 [PMID: 22284346 DOI: 10.1016/j.ejso.2011.12.021]
103 **Shapiro B**. Optimization of radioiodine therapy of thyrotoxicosis: what have we learned after 50 years? *J Nucl Med* 1993; **34**: 1638-1641 [-PMID: 8410274]
104 **Cosgriff PS.** Thyroid blocking associated with I123- and I131 MIBG scans. Available from: URL: http: //www.nuclearmedicine.org.uk/thyroid/thyweb.pdf
105 **Li JJ**, Cona MM, Feng YB, Chen F, Zhang GZ, Fu XB, Himmelreich U, Oyen R, Verbruggen A, Ni YC. A single-dose toxicity study on non-radioactive iodinated hypericin for a targeted anticancer therapy in mice. *Acta Pharmacol Sin* 2012; **33**: 1549-1556 [PMID: 23103619 DOI: 10.1038/aps.2012.111]
106 **Van Landeghem L**, Blue RE, Dehmer JJ, Henning SJ, Helmrath MA, Lund PK. Localized intestinal radiation and liquid diet enhance survival and permit evaluation of long-term intestinal responses to high dose radiation in mice. *PLoS One* 2012; **7**: e51310 [PMID: 23236468 DOI: 10.1371/journal.pone.0051310]
107 **Cona MM,** Feng Y, Verbruggen A, Oyen R, Ni Y. Improved clearance of radioiodinated hypericin as a targeted anticancer agent by using a duodenal drainage catheter in rats. *Exp Biol Med* (Maywood) 2013 Oct 21; Epub ahead of print [PMID: 24146264]
108 **Cona MM**, Li J, Chen F, Feng Y, Alpizar YA, Vanstapel F, Talavera K, de Witte P, Verbruggen A, Sun Z, Oyen R, Ni Y. A safety study on single intravenous dose of tetrachloro-diphenyl glycoluril [iodogen] dissolved in dimethyl sulphoxide (DMSO). *Xenobiotica* 2013; **43**: 730-737 [PMID: 23294333 DOI: 10.3109/00498254.2012.756559]
109 **Ell PJ**, Langford R, Pearce P, Lui D, Elliott AT, Woolf N, Williams ES. 99mTc-imidodiphosphonate: a superior radiopharmaceutical for in vivo positive myocardial infarct imaging. I: Experimental data. *Br Heart J* 1978; **40**: 226-233 [PMID: 637975 DOI: 10.1136/hrt.40.3.226]
110 **Obrador D**, Ballester M, Carrió I, Augé JM, López CM, Bosch I, Martí V, Bordes R. Active myocardial damage without attending inflammatory response in dilated cardiomyopathy. *J Am Coll Cardiol* 1993; **21**: 1667-1671 [PMID: 8496535 DOI: 10.1016/0735-1097(93)90385-E]
111 **Dec GW**, Palacios I, Yasuda T, Fallon JT, Khaw BA, Strauss HW, Haber E. Antimyosin antibody cardiac imaging: its role in the diagnosis of myocarditis. *J Am Coll Cardiol* 1990; **16**: 97-104 [PMID: 2358612 DOI: 10.1016/0735-1097(90)90463-Y]
112 **Frist W**, Yasuda T, Segall G, Khaw BA, Strauss HW, Gold H, Stinson E, Oyer P, Baldwin J, Billingham M. Noninvasive detection of human cardiac transplant rejection with indium-111 antimyosin (Fab) imaging. *Circulation* 1987; **76**: V81-V85 [PMID: 3311460]
113 **Buja LM**, Tofe AJ, Kulkarni PV, Mukherjee A, Parkey RW, Francis MD, Bonte FJ, Willerson JT. Sites and mechanisms of localization of technetium-99m phosphorus radiopharmaceuticals in acute myocardial infarcts and other tissues. *J Clin Invest* 1977; **60**: 724-740 [PMID: 893676 DOI: 10.1172/JCI108825]
114 **Khaw BA**, Nakazawa A, O'Donnell SM, Pak KY, Narula J. Avidity of technetium 99m glucarate for the necrotic myocardium: in vivo and in vitro assessment. *J Nucl Cardiol* 1997; **4**: 283-290 [PMID: 9278874 DOI: 10.1016/S1071-3581(97)90105-7]
115 **Hiroe M**, Ohta Y, Fujita N, Nagata M, Toyozaki T, Kusakabe K, Sekiguchi M, Marumo F. Myocardial uptake of 111In monoclonal antimyosin Fab in detecting doxorubicin cardiotoxicity in rats. Morphological and hemodynamic findings. *Circulation* 1992; **86**: 1965-1972 [PMID: 1451268 DOI: 10.1161/01.CIR.86.6.1965]
116 **Bianco JA**, Kemper AJ, Taylor A, Lazewatsky J, Tow DE, Khuri SF. Technetium-99m(Sn2+)pyrophosphate in ischemic and infarcted dog myocardium in early stages of acute coronary occlusion: histochemical and tissue-counting comparisons. *J Nucl Med* 1983; **24**: 485-491 [PMID: 6854398]
117 **Khaw BA**, Strauss HW, Moore R, Fallon JT, Yasuda T, Gold HK, Haber E. Myocardial damage delineated by indium-111 antimyosin Fab and technetium-99m pyrophosphate. *J Nucl Med* 1987; **28**: 76-82 [PMID: 3025386]
118 **Fonge H**, Vunckx K, Wang H, Feng Y, Mortelmans L, Nuyts J, Bormans G, Verbruggen A, Ni Y. Non-invasive detection and quantification of acute myocardial infarction in rabbits using mono-[123I]iodohypericin microSPECT. *Eur Heart J* 2008; **29**: 260-269 [PMID: 18156139 DOI: 10.1093/eurheartj/ehm588]
119 **Cona MM**, Feng Y, Li Y, Chen F, Vunckx K, Zhou L, Van Slambrouck K, Rezaei A, Gheysens O, Nuyts J, Verbruggen A, Oyen R, Ni Y. Comparative study of iodine-123-labeled hypericin and 99mTc-labeled hexakis [2-methoxy isobutyl isonitrile] in a rabbit model of myocardial infarction. *J Cardiovasc Pharmacol* 2013; **62**: 304-311 [PMID: 23714775 DOI: 10.1097/FJC.0b013e31829b2c6b]
120 **Vorvick LJ,** Longstreth GF, Zieve D. Acute cholecystitis. *MedlinePlus* 2011. Available from: URL: http: //www.nlm.nih.gov/medlineplus/ency/article/000264.htm
121 **Csendes A**, Burdiles P, Maluenda F, Diaz JC, Csendes P, Mitru N. Simultaneous bacteriologic assessment of bile from gallbladder and common bile duct in control subjects and patients with gallstones and common duct stones. *Arch Surg* 1996; **131**: 389-394 [PMID: 8615724 DOI: 10.1001/archsurg.1996.01430160047008]
122 **Pañella H**, Rius C, Caylà JA. Transmission of hepatitis C virus during computed tomography scanning with contrast.

Emerg Infect Dis 2008; **14**: 333-336 [PMID: 18258135 DOI: 10.3201/eid1402.060763]

123 **Chen KT**, Chen CJ, Chang PY, Morse DL. A nosocomial outbreak of malaria associated with contaminated catheters and contrast medium of a computed tomographic scanner. *Infect Control Hosp Epidemiol* 1999; **20**: 22-25 [PMID: 9927261 DOI: 10.1086/501557]

124 **Cantin V**, Labadie R, Rhainds M, Simard FC. Intravenous contrast medium administration in computerized axial tomography at the CHUQ Medical Imaging Department. Centre hospitalier universitaire de Québec 2007. Available from: http://www.chuq.qc.ca/NR/rdonlyres/03BC97EF-5F04-4375-BC48-3852965A4EDD/0/R%C3%89SUM%C3%89substancedecontrasteVArevised_VF.pdf.Accessed%20Nov%2029,%202010

125 **Cona MM**, Bauwens M, Zheng Y, Coudyzer W, Li J, Feng Y, Wang H, Chen F, Verbruggen A, Oyen R, Ni Y. Study on the microbial safety of an infusion set for contrast-enhanced imaging. *Invest Radiol* 2012; **47**: 247-251 [PMID: 22353856 DOI: 10.1097/RLI.0b013e31823c0f87]

P- Reviewers: Guo ZS, Leitman IM **S- Editor**: Ma YJ
L- Editor: Wang TQ **E- Editor**: Wu HL

百世登
Baishideng®

Published by **Baishideng Publishing Group Co., Limited**
Flat C, 23/F., Lucky Plaza, 315-321 Lockhart Road,
Wan Chai, Hong Kong, China
Fax: +852-65557188
Telephone: +852-31779906
E-mail: bpgoffice@wjgnet.com
http://www.wjgnet.com